

OPEN ACCESS

EDITED BY
Cristiana Moreira,
University of Porto, Portugal

REVIEWED BY
Cristiane Cassiolato Pires Hardoim,
São Paulo State University, Brazil
Diogo Antonio Tschoeke,
Federal University of Rio de Janeiro, Brazil

*CORRESPONDENCE
Marie-Lise Bourguet-Kondracki
✉ marie-lise.bourguet@mnhn.fr
Sébastien Duperron
✉ sebastien.duperron@mnhn.fr

RECEIVED 06 April 2023
ACCEPTED 04 July 2023
PUBLISHED 31 July 2023

CITATION
Wang H, Halary S, Duval C, Bernard C,
Troussellier M, Beniddir MA, Brunel J-M,
Castaldi A, Caudal F, Golléty C, Martin C,
Bourguet-Kondracki M-L and Duperron S
(2023) Diversity, metabolome profiling and
bioactivities of benthic filamentous
cyanobacteria isolated from coastal
mangroves of Mayotte.
Front. Mar. Sci. 10:1201594.
doi: 10.3389/fmars.2023.1201594

COPYRIGHT
© 2023 Wang, Halary, Duval, Bernard,
Troussellier, Beniddir, Brunel, Castaldi,
Caudal, Golléty, Martin, Bourguet-Kondracki
and Duperron. This is an open-access article
distributed under the terms of the [Creative Commons Attribution License \(CC BY\)](https://creativecommons.org/licenses/by/4.0/). The
use, distribution or reproduction in other
forums is permitted, provided the original
author(s) and the copyright owner(s) are
credited and that the original publication in
this journal is cited, in accordance with
accepted academic practice. No use,
distribution or reproduction is permitted
which does not comply with these terms.

Diversity, metabolome profiling and bioactivities of benthic filamentous cyanobacteria isolated from coastal mangroves of Mayotte

Huibin Wang¹, Sébastien Halary¹, Charlotte Duval¹,
Cécile Bernard¹, Marc Troussellier², Mehdi A. Beniddir³,
Jean-Michel Brunel⁴, Andrea Castaldi^{1,5}, Flore Caudal^{5,6},
Claire Golléty⁷, Coralie Martin¹,
Marie-Lise Bourguet-Kondracki^{1*} and Sébastien Duperron^{1*}

¹UMR 7245 MCAM, Muséum National d'Histoire Naturelle, Paris, France, ²MARBEC, Univ Montpellier, CNRS, IFREMER, IRD, Montpellier, France, ³Équipe "Chimie des Substances Naturelles" BioCIS, CNRS, Université Paris-Saclay, Orsay, France, ⁴UMR MD1, U-1261, Aix Marseille Université, INSERM, SSA, MCT, Marseille, France, ⁵Laboratoire de Biotechnologie et Chimie Marines, Université Bretagne Sud, EMR CNRS 6076, IUEM, Lorient, France, ⁶IRD, Univ Brest, CNRS, Ifremer, LEMAR, Plouzane, France, ⁷MARBEC, Univ Montpellier, CNRS, IFREMER, IRD, Montpellier, CUFR de Mayotte, Dembeni, France

Introduction: Cyanobacteria are important members of the dense biofilms that colonize available substrates in mangrove habitats worldwide. However, their taxonomic diversity and biological activities have received little attention.

Methods: The occurrence of cyanobacteria is evaluated in 27 biofilms collected from mangroves in Mayotte. Filamentous cyanobacterial strains were isolated and characterized using 16S rRNA comparative gene sequence analysis. LC-MS/MS experiments were performed on the crude extracts of the faster-growing strains, and construction of their molecular network showed a conspectus of their chemical diversity. Biological activities of the strain extracts were then evaluated using standard assays.

Results and discussion: Isolation procedures yielded 43 strains representing 22 species-level taxa, of which only three could be assigned to existing species. Some of these strains were among the most abundant cyanobacteria present in biofilms. PCR assays did not support the production of the major cyanotoxins. Analysis of metabolites from 23 strains using both in silico tools ISDB- DNP (In silico Data Base–Dictionary of Natural Products) and MolDiscovery, revealed occurrence of godavarin K, a limonoid natural product previously isolated from the seeds of an Indian mangrove tree. This annotation was further confirmed by the marine database MarinLit, suggesting that cyanobacteria might be an alternative source of godavarin K and its four isomers. While no significant antimicrobial and cytotoxic activities were observed, some strains exhibited

anthelmintic and antibiofilm activities that warrant further investigation and may be relevant to biofilm ecology. Mangrove biofilms thus appear to be an untapped reservoir of novel culturable cyanobacterial lineages, with bioactivities relevant to their biofilm lifestyle, which may be of interest for bioinspiration.

KEYWORDS

benthic cyanobacteria, mangrove, Mayotte, phylogenetic diversity, biofilms, chemical diversity, molecular networking, biological activities

1 Introduction

Cyanobacteria are among the most important primary producers in terrestrial, freshwater, and marine ecosystems. They are dominant members of the phytoplankton in aquatic environments but they can also be abundant in biofilms attached to sediment, biological surfaces, as well as rocks (Meyer et al., 2017b; Petrescu and Ungureanu, 2022). In tropical areas, biofilm-forming cyanobacteria can contribute significantly to the local trophic network by fixing carbon and nitrogen, and providing various necessary nutrients (Rocha et al., 2020; Busi et al., 2022). Cyanobacteria-containing biofilms are particularly abundant in mangroves, where they can cover extensive areas on a variety of substrates (Alvarenga et al., 2015), and may play important ecological roles, such as carbon sinks (Nellemann et al., 2009; Bulseco et al., 2020), or feed for fish nurseries that can involve economically-important species (Aburto-Oropeza et al., 2008). However, the composition of biofilms, identity of cyanobacterial members, as well as their characteristics and importance for the productivity of mangrove ecosystems, remain poorly studied (Bhadury and Singh, 2020). In addition to being ecologically important microorganisms, cyanobacteria are also producers of a wide range of bioactive secondary metabolites (Welker and Von Döhren, 2006; Demay et al., 2019), including cyanotoxins (Sanseverino et al., 2017) and various antibacterial molecules that affect their interactions with other organisms, making them a target group for biotechnology (Tan and Phyo, 2020; Wang et al., 2020; Petrescu and Ungureanu, 2022). Some of these molecules are already used in medicine, such as in Brentuximab vedotin (Caldora-based dolastatin 10), which is used to treat Hodgkin lymphoma (Tan and Phyo, 2020; Wang et al., 2020).

Currently, the ~ 1,700 cyanobacterial species (Komárek et al., 2014) described so far represent a small fraction of the estimated taxonomic diversity of the group. Compared to pelagic species, the benthic compartment, in particular in tropical regions, is significantly under-explored (Duperron et al., 2020). In addition to identifying new species based on morphology and molecular taxonomical approaches, metabolomics methods allow researchers to delve deeper into the chemical diversity of cyanobacteria by focusing on the diversity of the metabolites they produce. Until 2019, more than 50% of the characterized cyanobacterial metabolites were identified from the order Oscillatoriales, and 35% from the sole genus *Lyngbya*

(Demay et al., 2019), highlighting the potential chemical diversity to be found in new species.

In this study, we investigated the cyanobacterial diversity from several biofilms collected in three mangroves located on the main island of Mayotte (Grande-Terre). Mangroves are coastal forests, and despite abundant primary production, they are generally considered oligotrophic with low organic matter, N and P contents, due to massive tide-mediated nutrient export (Reef et al., 2010; Adame et al., 2014). However, their productivity often exceeds $1\text{kg}\cdot\text{m}^{-2}\cdot\text{yr}^{-1}$ (Blasco et al., 1996). Aside from plants, photoautotrophic microorganisms are likely to be significant contributors to this productivity.

Different types of biofilms likely to contain cyanobacteria were collected on sediment or attached to the bark of mangrove trees' roots and trunks in three sites of Mayotte. The composition of biofilm prokaryotic communities was analyzed using a 16S rRNA gene sequencing approach. Filamentous cyanobacterial strains were isolated and identified using 16S rRNA comparative gene sequence analysis and morphological characteristics. The potential for cyanotoxin production was evaluated based on PCR assays. The chemical diversity of metabolites was profiled by LC-MS/MS experiments on extracts of isolated strains and molecular network analysis. A first screening of biological activities of strain metabolites was performed by analyzing antibacterial activities against Gram-positive *Staphylococcus aureus*, *Enterococcus faecalis*, and Gram-negative *Escherichia coli*, *Pseudomonas aeruginosa*, and cytotoxic activities against CHO (Chinese hamster ovary) cells. In addition, antibiofilm and anthelmintic activities were investigated using extracts of isolated strains. This research provides a first glimpse of the composition of the biofilms, as well as the taxonomic and chemical diversity, and bioactivities of culturable benthic filamentous cyanobacteria occurring in the coastal mangroves of Mayotte.

2 Materials and methods

2.1 Biofilm sampling and cyanobacteria strains isolation

Biofilms presumed to contain abundant cyanobacteria based on their green-to-brown color, were sampled in three mangroves on

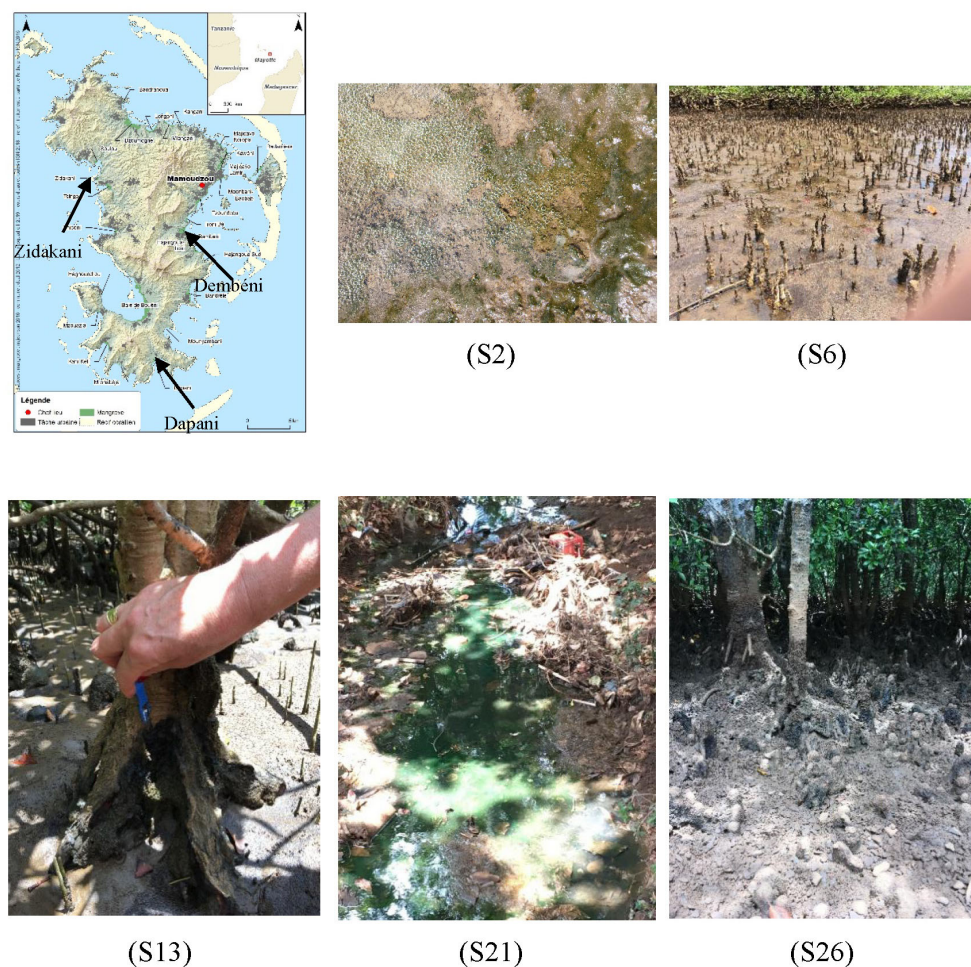


FIGURE 1
Location of Dembeni, Zidakani, and Dapani mangroves in Mayotte, and types of biofilms sampled on different substrates including sediment (S2), roots (S6, S26), tree bark (S13), a temporary river (S21).

the Mayotte island of Grande-Terre: Dembeni (areas 1 and 2, 20 biofilms), Zidakani (4 biofilms), and Dapani (3 biofilms) between November 8th and 11th, 2018 (Table S1; Figure 1). Biofilms, either benthic or attached to substrates including mangrove tree bark and debris were sampled using sterile tweezers, photographed, and transferred to sterile Falcon tubes in a cooler. Following Article 17, paragraph 2, of the Nagoya Protocol on Access and Benefit-sharing, a sampling permit was issued and published (<https://absch.cbd.int/database/ABSCH-IRCC-FR-246969>).

Back to the laboratory, biofilm samples were split. One fragment was stored in RNAlater™ (Ambion, UK) then frozen for DNA extraction. Another fragment was observed under a microscope. Cyanobacteria-rich fractions from 25 of the 27 biofilms were sampled using a Pasteur pipette under the microscope and inoculated on solid (5 g.L⁻¹ agar) Z8 culture medium, either as is, or containing 20 g.L⁻¹ of salt (Instant Ocean) (Rippka, 1988). Single filaments were isolated by repeated transfers on liquid media under an inverted microscope (Nikon ECLIPSE TS100), with or without cycloheximide to prevent fungi growth.

2.2 DNA extraction and 16S rRNA metabarcoding of biofilms

DNA was extracted from the 27 biofilms using the ZymoBIOMICS DNA mini kit (Zymo Research, CA) according to the manufacturer's instructions, after a disruption step using glass beads (6 x 1min, 30 Hz, 1,800 oscillations per minute). A ~ 400 bp fragment of the rRNA-encoding gene corresponding to the V4-V5 variable region of *Escherichia coli* was amplified using primers 515F and 926R (Fadeev et al., 2021) and sequenced on an Illumina MiSeq platform (2x300 bp, paired end, Genoscreen, France). Company-provided mock communities of known composition were used as an internal control for the whole sequencing process. Raw reads were deposited into the GENBANK Sequence Read Archive (SRA, Bio project PRJNA947804).

Sequence reads were analyzed using QIIME2 (Hall and Beiko, 2018). Amplicon Sequence Variants (ASVs) (Fadeev et al., 2021) were identified using DEBLUR (Amir et al., 2017) using default parameters, i.e. a maximal probability for indels of 0.01 and mean read error rate of 0.5% for normalization. Chimeric sequences were

identified using UCHIME (Mühr et al., 2020) and then removed (Edgar et al., 2011), and the taxonomic affiliations were obtained by using the sklearn-based classifier (GreenGenes 13-8-99 release). Sequences matching “Eukaryota”, “Chloroplast” and “Mitochondria” were discarded. Representative plots were obtained using GGPlot2.

2.3 Strains cultivation and biomass production

Isolated strains and cultures were all monoclonal and non-axenic. A total of 43 strains were registered in the Muséum national d’Histoire naturelle (MNHN, Paris, France) culture collection of cyanobacteria and microalgae, where they are available upon request (<https://www.mnhn.fr/fr/microalgues-et-cyanobacteries>) (Hamlaoui et al., 2022), under labels PMC (Paris Museum Collection) 1096.18 to PMC 1143.19 (Table 1). Biomass was generated for further characterization by culturing strains in increasing volumes of liquid Z8 medium (25°C; 15 $\mu\text{mol.m}^{-2}.\text{s}^{-1}$ white light; 16 h light; 8 h dark) without salt (PMC 1097.19, PMC 1099.19, PMC 1100.19, PMC 1101.19, PMC 1104.19 to PMC 1106.19, PMC 1111.19 to PMC 1115.19, PMC 1134.19,

PMC 1136.19, PMC 1140.19) or with 20 g.L^{-1} salt (other strains) for two months, depending on which conditions were leading to increased growth. The morphological characteristics (such as filament diameter, presence of heterocytes, akinetes, constrictions between cells) of strains were subsequently observed under the inverted microscope (Nikon ECLIPSE TS100, Japan).

2.4 Strains identification using 16S rRNA sequencing and PCR assay for genes involved in cyanotoxin production

DNA was extracted from cultures using the ZymoBIOMICS Fecal/Soil Kit (Zymo Research, Irvine, CA, USA), after a 3-minute disruption of cells with ceramic beads, using reagents and conditions as described in the manufacturer’s instructions (Ammar et al., 2014), and concentration was measured using Nanodrop and Qubit. Cyanobacteria 16S rRNA encoding genes were PCR amplified (35 cycles) using two targeted primer sets designed for this group. The annealing temperature of 58°C was used for primer set 8F (5'-AGAGTTTGATCCTGGCTCAG-3') and 920R (5'-TTGTAAGGTTCTTCGCGTTG-3'), and annealing at 55°C was used for primer set 861F (5'-TAACGCGTTAAGTATCCC-3') and 1380R (5'-TAACGACTTCGGGCGTGACC-3') (Gugger et al., 2002; Ludwig, 2007).

TABLE 1 Cyanobacterial strains isolated from Mayotte habitats (Table S1).

Strain ID	Order	Affiliation	Isolation sample	Difference between ASV and strains sequence (bp vs. 345bp)	Samples displaying ASVs (% among cyanobacterial/% among total bacterial reads)*	Best BLAST sequence
PMC 1096-1098	Coleofasciculales	<i>Symploca</i> , sp. 1	S2	1	S2 (60.7/19.7)	<i>Symploca</i> sp. HBC5 (EU249122)
PMC 1097-1099	Nostocales	<i>Hapalosiphon welwitschii</i>	S2		Nf	<i>Hapalosiphon welwitschii</i> UH IC-52-3 (KJ767019)
PMC1100-1112-1113-1114-1115	Oscillatoriales	<i>Planktothrix mougeotii</i>	SS21	0-1	S21 (94.5%/44.4%)	<i>Planktothrix mougeotii</i> HAB002 (FJ184392)
PMC 1101	Nostocales	<i>Brasilonema</i> , sp.	S15	4	S15 (27.1%/5.1%)	<i>Brasilonema terrestre</i> strain CENA116 (NR116034)
PMC 1102-1103-1116	Oscillatoriales	<i>Hydrocoleum</i> , sp.	S17,S22	0-1	S17 (20.1%/4.3%)/S30 (0.3%/0.1%)	<i>Hydrocoleum lyngbyaceum</i> HBC7 (EU249124)
PMC 1104-1105	Oscillatoriales	<i>Capilliphycus salinus</i>	S17	0-1	S17 (1.7%/0.2%)	<i>Capilliphycus salinus</i> ALCB114379 (NR176504)
PMC 1108.19	Oscillatoriales	<i>Dapis</i> , sp.	S18		Nf	<i>Dapis pnigousa</i> NAB11-4 (MF061806)
PMC 1109.19	Leptolyngbyales	<i>Jaaginema</i> , sp.	S18		Nf	<i>Jaaginema</i> sp. PMC 1073.18 (MN823180)
PMC 1110-1111	Spirulinales	<i>Spirulina</i> , sp. 1	S18		Nf	<i>Spirulina major</i> 0BB22S09 (AJ635436)

(Continued)

TABLE 1 Continued

Strain ID	Order	Affiliation	Isolation sample	Difference between ASV and strains sequence (bp vs. 345bp)	Samples displaying ASVs (% among cyanobacterial/% among total bacterial reads)*	Best BLAST sequence
PMC 1117	Synechococcales	<i>Halomicronema</i> sp.	S22	0	S22 (0.8%/0.1%)	Uncultured cyanobacterium clone BP2015-16 (MH084964)
PMC 1119-1121-1127-1137	Oscillatoriales	<i>Capilliphycus</i> sp.	S23		Nf	Uncultured bacterium clone SIUS518 (JX002457)
PMC 1122	Coleofasciculales	<i>Coleofasciculus</i> sp.	S23		Nf	Uncultured organism clone SBYB-990 (JN439618)
PMC 1123	Coleofasciculales	<i>Symploca</i> sp. 2	S23	2	S9 (1.3%/0.3%)/S10 (0.2%/0.03%)/S22 (0.3%/0.03%)	<i>Symploca</i> sp. HBC5 (EU249122)
PMC 1124	Synechococcales	Gen. Nov. 1, sp.	S23	3	S17 (0.03%/0.006%)/S22 (0.16%/0.01%)/S23 (100%/7.9%)/S6 (0.6%/0.1%)	<i>Leptolyngbya valderiana</i> BEA 0039B (ON032977)
PMC 1125	Synechococcales	<i>Thainema</i> sp. 1			Nf	Synechococcales cyanobacterium PMC 1067.18 (MW432541)
PMC 1126.19	Synechococcales	<i>Thainema</i> sp. 2	S23	3	S9 (2.8%/0.6%)/S10 (0.3%/0.04%)	Synechococcales cyanobacterium PMC 1067.18 (MW432541)
PMC 1129-1130-1133	Oscillatoriales	Gen. Nov. 2, sp.	S27	0	S27 (0.1%/0.06%)	Uncultured cyanobacterium partial (FM242281)
PMC 1131-1132-1134	Oscillatoriales	<i>Neolyngbya</i> sp.	S27	0	S2 (0.04%/0.01%)/S14-2 (0.5%/0.02%)/S27 (78.0%/42.5%)	<i>Neolyngbya irregularis</i> ALCB 114389 (MF190470)
PMC 1135.19	Oscillatoriales	Gen. Nov. 3, sp.	S29		Nf	<i>Bacterium</i> YC-ZSS-LKJ29 (KP174505)
PMC 1136-1139	Nostocales	<i>Wollea</i> sp. 1	S29	0	S29 (9.4%/5.5%)	<i>Sphaerospermopsis</i> sp. CENA247 (MN551909)
PMC 1138-1140	Nostocales	<i>Wollea</i> sp. 2	S29	0-3	S29 (28.1%/16.4%)	<i>Hetercystous cyanobacterium</i> RS0112 (KY038574)
PMC 1141-1142-1143	Spirulinales	<i>Spirulina</i> sp. 2	S29		Nf	Uncultured organism clone SBXZ_5386 (JN436532)

Strain ID corresponds to the reference number in the Paris Museum Collection (PMC) of cyanobacteria from which strains are available upon request. Affiliation is according to the 16S rRNA-based phylogenetic analysis displayed in Figures 2–4 and to the distance matrix in Table S2. Nf: ASV was not found.

Both amplicons were sequenced and sequence chromatograms (Genoscreen, Lille, France) were analyzed, assembled by Geneious (<https://www.geneious.com/>) for each strain, and compared to the GENBANK database with BLAST (default parameters, standard databases, optimize for highly similar sequences program selected). Sequences were submitted to GENBANK under accession numbers OQ693634 to OQ693681.

A dataset was constructed consisting of sequences of the 43 isolated strains, their best BLAST hits, and representatives of major cyanobacterial lineages. Sequences were aligned by the secondary structure-aware Silva tool [Ribosomal Database Project website

(Cole et al., 2009)]. After alignment, ambiguously aligned regions were deleted using Bioedit 7.2.5. Phylogenetic relationships were inferred using a Maximum Likelihood approach based on General Time Reversible Model (5 categories and invariants, see tree captions for details, selected based on the Akaike Information) (Posada and Buckley, 2004). A pairwise p-distance matrix (Table S2) was generated to aid preliminary genus and species delimitation. Phylogenetic trees were constructed by using the software MEGA 7 (Newman et al., 2016).

The presence of four genes diagnostic to produce microcystin, anatoxin, cylindrospermopsin, and saxitoxin families, respectively,

was tested using specific primer sets and PCR programs on all strains (Table S3).

2.5 Identification of abundant strains in natural biofilms

The 16S rRNA-encoding genes sequences obtained from all 43 strains were compared with ASVs obtained from the 27 biofilms to evaluate the relative abundance of isolated strains in natural biofilms. For this, cyanobacterial ASVs were extracted from biofilm datasets and aligned with strain sequences using Clustal W. Number of differences between most similar ASVs and strains were computed based on a 345 bp alignment. ASVs displaying 3 or fewer differences with strain sequences (~1%) were retained, and their respective abundance versus bacterial and cyanobacterial sequences in biofilm samples were checked. All analyses were conducted using MEGA-7 (Newman et al., 2016).

2.6 Preparation of cyanobacteria chemical extracts

Chemical extracts were performed for the 23 strains for which enough biomass was available after two months. Each culture sample was stored in 50 mL Falcon tubes, containing 40 mL salt-free Z8 medium. After centrifugation at 4,000 g, three deep washes with unsalted Z8 medium were done, then the supernatant was discarded, and the cyanobacteria pellets were lyophilized under vacuum at -40°C for 12 h after freezing at -80°C for 30 minutes. Dry biomass was weighted, and 20 mg were re-suspended in a 2 mL solvent mixture consisting of MeOH/CH₃CN/H₂O (40:40:20). After three successive cycles of sonication (6 min cycle: 1 min ON; 30 s OFF) and centrifugations (14,000 g, 5 min), supernatants were evaporated and the dry crude extracts were weighed and suspended in MeOH (1 mg. mL⁻¹). Finally, extracts were filtered on a 0.2 μm membrane (4 mm in diameter Phenomenex®). An aliquot of 30 μL was reserved for LC-MS/MS analysis. The rest of the crude extract samples was evaporated and diluted in DMSO (1 μg. μL⁻¹), after which 200 μL aliquots were used for activities assay.

2.7 LC-MS/MS data-dependent acquisition and processing

UPLC-HRMS/MS analyses were achieved by coupling a LC system to a hybrid quadrupole-time-of-flight mass spectrometer Agilent 6546 equipped with an ESI source, operating in positive-ion mode. The UPLC (C18 BEH Acquity® Waters 100 × 2.1 mm, 1.7 μm column, 500 μL.min⁻¹ gradient elution (A: CH₃CN, B: H₂O + 0.1% formic acid) from 5% to 100% A, over 12 min) was used to perform chromatographic separation. Source parameters were set as followed: capillary temperature at 320°C, source voltage at 3500 V, and sheath gas flow rate at 11 L.min⁻¹. MS scans were operated in full-scan mode from *m/z* 100 to 1200 (0.1 s scan time) with a mass

resolution of 60,000 at *m/z* 922. In the positive-ion mode, purine C₅H₄N₄ [M+H]⁺ ion (*m/z* 121.050873) and the hexakis (1H,1H,3H-tetrafluoropropoxy) phosphazene C₁₈H₁₈F₂₄N₃O₆P₃ [M+H]⁺ ion (*m/z* 922.009798) were used as internal lock masses. A permanent MS/MS exclusion list criterion was set to prevent oversampling of the internal calibrant. LC-UV and MS data acquisition and processing were performed using MassHunter® Workstation software. Acquisition was performed in “Auto MS/MS” mode on the range *m/z* 100–1200 with an MS rate of 1 spectra.sec⁻¹ and an MS/MS scan rate of 3 spectra.sec⁻¹. Isolation MS/MS width was 1.3 *m/z*. Fixed collision energies of 45 eV was used. MS/MS events were performed on the four most intense precursor ions per cycle with a minimum intensity of 5,000 counts.

The MS data were converted from d (Agilent) standard data format to mzXML format by using the MSConvert software, part of the ProteoWizard package (Myers et al., 2017). Then, the converted mzXML files were processed with the MZmine software package v. 2.38 (Pluskal et al., 2010). The parameters were selected as follows: for mass detection, the centroid mass detector was utilized, with the noise level set to 2.5E3 for MS level 1 and 1.0E1 for MS level 2. The ADAP chromatogram (Du et al., 2020) builder was used, with a minimum group size of 4 scans, a 2.5E3 minimum group intensity threshold, a 1.0E3 minimum highest intensity, and a 10.0 ppm *m/z* tolerance. The wavelets approach was utilized for chromatogram deconvolution (ADAP). With a signal-to-noise ratio of 10, a minimum feature height of 1,000, a coefficient area threshold of 10, a peak duration range of 0.01 to 0.45 min, and an RT wavelet range of 0 to 0.1 min, the intensity window S/N was utilized as a S/N estimator. The isotope peaks grouper was used to detect isotopes with a *m/z* tolerance of 10.0 ppm, an RT tolerance of 0.3 min (absolute), a maximum charge of 1, and the most intense representative isotope employed. The join alignment method was used to align the peaks (*m/z* tolerance of 10 ppm, RT tolerance of 0.12 min). The weight of *m/z* was set as 50, the weight was set as 50, and the charge state must be the same. The same RT and *m/z* range gap filler was used to fill in the gaps in the peak list (*m/z* tolerance at 10 ppm, the retention time range 0.04 from 15.7 min). Finally, using the peak-list rows filter option, the aligned peak list was filtered to maintain only features linked with MS2 scans. LC-MS/MS data were deposited on MassIVE under the accession number: MSV000091466.

2.8 Molecular networks generation and annotation

A feature-based molecular network was generated using Global Natural Products Social Molecular Networking (GNPS) (Pluskal et al., 2010; Wang et al., 2016; Nothias et al., 2020) (<https://gnps.ucsd.edu/ProteoSAFe/static/gnps-splash.jsp>). The edges of the network were filtered to have a cosine score greater than 0.6 and more than six matched peaks. Further edges between two nodes were preserved in the network if and only if each node was in the top 10 most similar nodes of the others. The network's spectra were compared to GNPS' spectral libraries. All network spectra and library spectra match had to have a score of at least 0.6 and at least

six matched peaks. The molecular network was visualized using Cytoscape 3.9.1 software (Doncheva et al., 2019). The GNPS job parameters and resulting data are available at the following address (<https://gnps.ucsd.edu/ProteoSAFe/status.jsp?task=5bd14c218bdf4a799d6fe98cb8880d20>). The DEREPLICATOR annotation resulting data are available at the following address (<https://gnps.ucsd.edu/ProteoSAFe/status.jsp?task=3b8d860a0b794769b25abe56d138ee34>). To extend the annotations, two additional *in silico* tools, namely ISDB (Allard et al., 2016) and MolDiscovery (Cao et al., 2021) were used. Regarding ISDB tool, the annotation parameters were set as follows: spectral score (cosine > 0.2), parent mass tolerance (0.002 Da), and a maximum of five candidate structures were proposed. For the MolDiscovery processes, the parameters were: Precursor Ion Mass Tolerance 0.01 Da, Fragment Ion Mass Tolerance 0.01 Da, Max Charge at 1, and Min Significant Score at 10.0. Results of MolDiscovery annotations are available at the following address: (<https://gnps.ucsd.edu/ProteoSAFe/status.jsp?task=5556da8361b74371b27ce1b260d34809>). For more in-depth annotation, SIRIUS 5.6.2 (Dührkop et al., 2015) were used, the parameters of exporting MZmine data to SIRIUS were set as: weighted average m/z merge mode, mean intensity merge node, expected mass deviation 10 ppm, cosine threshold 0%, peak count threshold 0%, isolation window offset 0 m/z, isolation window width 0 m/z.

2.9 Evaluation of cytotoxic activities

Crude extracts from 23 cyanobacteria strains were used to evaluate the cytotoxic activity against CHO (Chinese Hamster Ovary) cells. Cells were seeded in a 96-well microplate, 5,000 cells. well⁻¹ in a 200 µL culture medium (DMEM low glucose - PAN biotech, Germany) and maintained at 37°C and 5% CO₂/95% air for 24 hours. After the incubation period, each well was supplemented with 50 µL cyanobacterial extracts at a final concentration of 500.0, 250.0, 125.0, 62.5, 31.2, or 15.6 µg. mL⁻¹. For the fractions eluted from the LH-20 column chromatography, the final concentration in each well was 20.0 µg. mL⁻¹. Each concentration was tested in three replicates, and the experiment was repeated three times (Trang et al., 2021). Paclitaxel (Sigma-Aldrich, USA) was used as a positive control at concentrations ranging from 0.003 to 30 µg. mL⁻¹. After 48 hours, cells were dyed with the MTT assay, and the optical density was measured using a Microplate reader SpectraMax Plus384 (GMI, USA) at two wavelengths of 570 and 690 nm (Bich-Loan et al., 2021). The IC₅₀ values (the concentration of extract at which 50% of cell growth was inhibited) were calculated by Excel and GraphPad Prism 8 software.

2.10 Evaluation of anthelmintic activities

To investigate the activity against filarial nematodes, 200 blood-purified first stage larvae (microfilariae) of the rodent filarial nematode *Litomosoides sigmodontis* were cultured *in vitro* in

200 µL RPMI 1640 medium (Sigma Aldrich) supplemented with HEPES 25mM, 10% FCS, 1% penicillin/streptomycin/amphotericin at 37°C, 5% CO₂ (Townson et al., 1987; Hawryluk et al., 2022). Each batch of microfilaria received 2 µL (5 µg. µL⁻¹) of crude extract, or 2 µL of DMSO solution as a control. Each condition was in triplicate. The motility of microfilariae was assessed by determining the mean worm motility scores from 0 to 3, with 3 corresponding to normal movement and uncoiled worm; 2 to slow movement and uncoiled; 1 to twitch movement and uncoiled; and 0 corresponding to no motility (dead worm). Scores were determined 2h post- addition.

2.11 Evaluation of antibiofilm activities

The antibiofilm activity of the crude extracts was tested against biofilm-forming *Pseudomonas aeruginosa* MUC-N1 (Boukerb et al., 2020). The bacteria strains were cultured in 5 mL of LB medium (NaCl 10g/L, tryptone 10g/L and yeast extract 5g/L) at 37°C under orbital shaking at 125 rpm, overnight in triplicate. 200 µL of diluted culture adjusted to OD₆₀₀ of 0.05 in fresh test medium was inoculated in each well, except for the blank. Aliquots of cyanobacterial extract at c (concentration) = 50 µg. mL⁻¹ (1% DMSO) was added to the 200 µL *P. aeruginosa* suspensions.

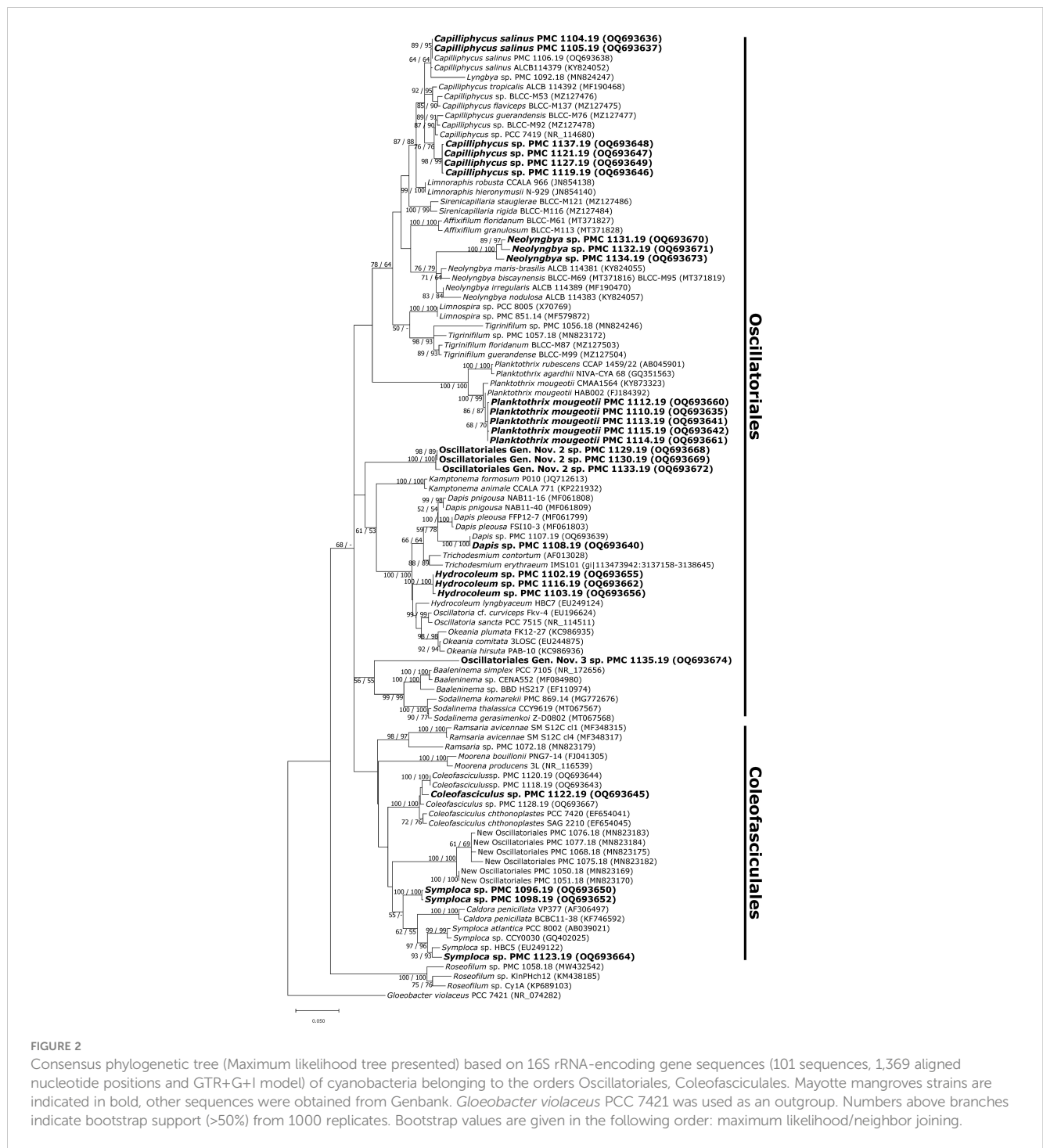
The 96-well microtiter plate (Thermo Scientific™ Nunc™ MicroWell™ 96-Well) was incubated in a stationary phase for 24 hours. After measuring the optical density at 600 nm (OD₆₀₀) using a TECAN Infinite M1000, the coloration and quantification of the biofilm was realized according to the Coffey & Anderson protocol (Coffey and Anderson, 2014), after acetic acid addition, by measuring the OD₅₅₀. The evaluation of the biofilm formation is corrected according to the growth of the bacteria strains. The values are presented as the mean ± SD. Data were evaluated with GraphPad Prism Version 8.01 software.

3 Results

3.1 Occurrence of cyanobacteria in biofilms

The composition of prokaryotic communities was analyzed from 27 biofilms collected from three mangroves in Mayotte (Table S1). Sampled biofilms occurred attached to sunken deadwood or debris (plastic, bamboo), covering the sediment surface, or adhering to mangrove tree roots and trunks (Figure 1). Sequencing of the V4-V5 region yielded a total of 1,119,200 quality-filtered sequences (44,414 ± 23,522 per biofilm). Apart from sample S23, which yielded only 339 reads with 189 ASVs, the 26 other samples yielded 26,334 to 85,074 reads clustering into 992 to 47,941 ASVs (11,452 ± 9,052 ASVs).

Bacteria were abundant in biofilms (Figure 5), with Alphaproteobacteria, Bacteroidota, Actinomycetota, and Cyanobacteria as the main taxa. The relative abundances of each taxon were highly variable among biofilms. Cyanobacteria represented between 1.35% (sample S26) and 61.07% (sample



S30, Table S1) of reads. Interestingly, biofilms that displayed evident blue-green colors, such as samples S2, S21, and the three samples from Dapani (S27, 29, and 30) displayed particularly high abundances of Cyanobacteria compared to samples that did not have a greenish appearance (e.g., samples S13 and S26 illustrated in Figure 1). Over the whole dataset, cyanobacteria clustered into 157 ASVs, each recovered from 1 to 5 biofilms. Of these ASVs, 15 represented at least 5% of all reads in at least one biofilm sample, and could be considered as abundant members of the biofilm (Tables 1, S1).

3.2 Isolation of cyanobacterial strains and taxonomic assignment to genera

A total of 43 cyanobacterial strains (Table 1) were isolated from 10 of the 27 biofilms and successfully maintained in the PMC culture collection. During growth, they formed extensive fasciculate mats or small clusters in the medium, with colors ranging from brown-green, olive-green to dark green (Figure 6). Analysis of the 16S rRNA-encoding gene sequences indicates that isolated strains belong to the cyanobacterial orders Oscillatoriales,

Nostocales, Spirulinales, Coleofasciculales, Synechococcales, and Leptolyngbyales (22, 7, 5, 4, 4 and 1 strains, respectively), (Sturnecky et al., 2023). Strains were assigned to existing species and genera based on widely accepted 16S rRNA similarity cutoff values of 98.65% and 95% similarity for the 16S rRNA-encoding gene, respectively (Kim et al., 2014; Komárek et al., 2014), on monophyly, and on morphological features (filament diameter, presence of heterocytes, sheath, akinetes, constrictions between cells) overall consistent with members of these genera. When no published species or genus sequence fell within this similarity range and with the support of phylogenetic reconstruction, strains were assigned to hypothetical species (sp.) and genera (gen. nov.) (Caires et al., 2018a; Caires et al., 2018b; Berthold et al., 2021).

Based on sequence similarity criteria, strains were grouped into 22 species-level taxa according to selected threshold values (Table 1; Table S2). Over half of the strains (26 out of 43 strains) belong to the orders Oscillatoriales and Coleofasciculales (Figure 2). Among these, seven strains correspond to two previously described species, namely *Capilliphycus salinus* (PMC 1104.19 and PMC 1105.19) and *Planktothrix mougeotii* (PMC 1100.19, PMC 1112.19, PMC 1113.19, PMC 1114.19, PMC 1115.19). The rest of the Oscillatoriales strains can be assigned to undetermined species within genera *Hydrocoleum* (PMC 1102.19, 1103.19, and 1116.19),

Capilliphycus (PMC 1119.19, 1121.19, 1127.19, and 1137.19), *Neolyngbya* (PMC 1131.19, 1132.19, and 1134.19), and *Dapis* (PMC 1108.19, Tables 1 and S2). Strain PMC 1135.19, showed a 6.1% dissimilarity to the closest identified *Sodalinema*, above the 5% dissimilarity threshold, and is not monophyletic with this genus (Tables 1, S2; Figure 2). For these reasons, it is assigned to a hypothetical new genus. Strains PMC 1129.19, 1130.19, and 1133.19 cluster together in the phylogenetic tree, with no named genus within the 5% similarity criterion, thus representing another new hypothetical genus. Coleofasciculales comprise strains PMC 1096.19, PMC 1098.19 (from Dembeni 1, sample S2), and PMC 1123.19 (Zidakani, sample S23) which clustered together in the phylogenetic tree, both groups representing distinct species-level taxa within genus *Symploca*, with which display 4.2% dissimilarity in the 16S rRNA sequence. One strain, PMC 1122.19, belong to genus *Coleofasciculus*.

Seven strains belonging to the order Nostocales were isolated (Table 1; Figure 3). Strains PMC 1097.19 and 1099.19 isolated from sample S2 were affiliated with *Hapalosiphon welwitschii* because of the 99% similarity in their 16S rRNA sequences, and their clustering within the tree of *H. welwitschii* (KJ 767019, Figure 3).

The four strains isolated from sample S29 (PMC 1136.19, 1138.19, 1139.19, and 1140.19) clustered into two distinct species-

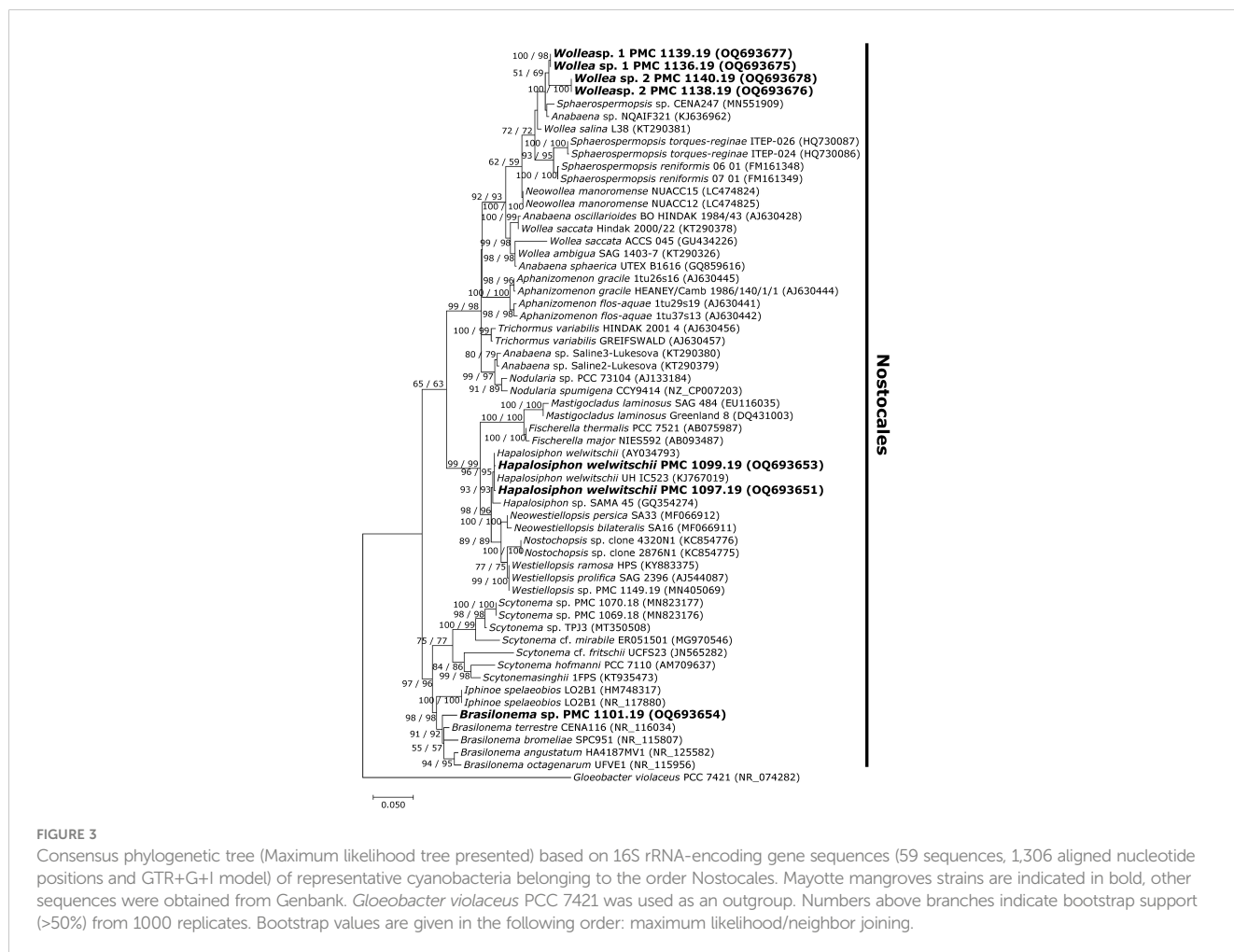




FIGURE 4 Consensus phylogenetic tree (Maximum likelihood tree presented) based on 16S rRNA-encoding gene sequences (68 sequences, 1,337 aligned nucleotide positions and GTR+G+I model) of cyanobacteria belonging to the orders Synechococcales, Leptolyngbyales, Spirulinales. Mayotte mangroves strains are indicated in bold, other sequences were obtained from Genbank. *Gloeobacter violaceus* PCC 7421 was used as an outgroup. Numbers above branches indicate bootstrap support (>50%) from 1000 replicates. Bootstrap values are given in the following order: maximum likelihood/neighbor joining.

level clades in the phylogenetic tree, with several closely related sequences from species belonging to genera *Wolleea*, *Anabaena* and *Sphaerospermopsis* (Figure 3). Their morphological characteristics include tubular colonies with common sheath, straight trichomes, organized parallel and tightly in colonies, and widely oval, most similar to those observed in *Wolleea* sp. (Kozlíková-Zapomělová et al., 2016) (Figure 6), and these were thus assigned to two distinct hypothetical species within this genus. Finally, strain PMC 1101.19 isolated from sample S15 was assigned to a hypothetical species within the genus *Brasilonema* with which it is monophyletic.

Using the same criteria, other species belonging to orders Spirulinales, Leptolyngbyales, and Synechococcales were assigned to hypothetical species (Figure 4). These belong to genera *Jaaginema* (PMC 1109.19), *Halomicronema* (PMC 1117.19), two distinct hypothetical species within genus *Thainema* (PMC 1125.19 and 1126.19 based on their 1.4% dissimilarity in the 16S rRNA-encoding gene), and two distinct species within genus *Spirulina* (PMC 1110.19 and 1111.19 in one species and PMC 1141.19, 1142.19 and 1143.19 in a second species), these latter two displaying the typical coiled morphology described in genus *Spirulina* (Figure 6). Strain PMC 1124.19 was assigned to a hypothetical new genus.

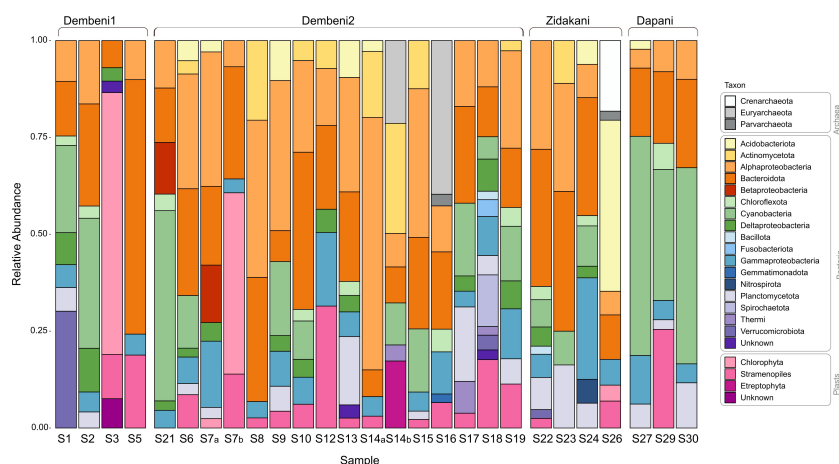


FIGURE 5
Taxa relative abundance in 27 biofilms sampled from mangroves in Mayotte.

PCR assays targeting genes involved in the production of microcystin, anatoxin, saxitoxin, and cylindrospermopsin yielded no amplicon for any of the 43 tested strains, despite that positive controls yielded amplicons (Table S3), suggesting absence of the target genes in their genomes.

3.3 Occurrence and relative abundance of identified species in natural biofilms

Out of the 22 species-level taxa identified among isolates, 13 were also identified as ASVs in 16S rRNA metabarcoding datasets obtained from 14 out of the 27 biofilms (Table 1). For 10 of these taxa, the corresponding ASV was recovered from at least one of the samples from which the strains were isolated. According to biofilm community compositions, eight species isolated in culture happened to be abundant members of the cyanobacterial community (i.e., they represented over 5% of cyanobacterial reads) in at least one biofilm sample. In several cases, the species was even the main cyanobacterial member of this biofilm, with taxon *Neolyngya* sp. (PMC 1132.19, 1134.10, 1131.19) representing 78.0% of the cyanobacterial reads in sample S27, taxon Gen. Nov. 1 sp. (PMC 1124.19) representing 100.0% in sample S23, *Symploca* sp. 1 (PMC 1096.19, 1098.19) representing 60.7% in S2 and *Planktothrix mougeoti* (PMC 1100.19, 1112.19, 1113.19, 1114.19, 1115.19) representing 94.5% in sample S21. Finally, seven isolated species were also abundant members of the whole community in at least one biofilm sample (i.e. they represented above 5% of all reads, Table 1).

3.4 MS/MS analysis and annotation of cyanobacterial specialized metabolites

Cultures from a total of 23 out of the 43 identified strains, representing 11 species-level taxa, yielded enough biomass for chemical characterization by LC-MS/MS analyses. To analyze the chemical diversity of the 23 extracts, LC-MS/MS experiments were

performed to enter the feature-based molecular networking workflow (Figure 7). A total of 2,667 features and 131 clusters were visualized in Cytoscape 3.9.1. The distribution of cyanobacterial metabolites among the 23 extracts of the entire molecular network was mapped at the genus level using a representative color tag. Analysis of the network showed that some molecular clusters were restricted to specific genera, highlighting the distribution of closely related compounds (Figure S1). The GNPS spectral library search yielded only eight hits including triphenylphosphate, triphenylphosphine, and pheophytin (https://gnps.ucsd.edu/ProteoSAFe/result.jsp?task=5bd14c218bdf4a799d6fe98cb8880d20&view=view_all_annotations_DB). As a way to enlarge the annotation coverage, DEREPLICATOR algorithm was used, which surprisingly failed to annotate any natural peptides. Nevertheless, two other *in silico* annotation tools ISDB and Moldiscovery allowed the annotation of 184 and 318 nodes respectively. They were mapped as red rectangles and shaped as triangles on the network, respectively (Figure S1; Tables S4, S5). Interestingly, 51 nodes were annotated by both tools, and thus appeared as red triangles on the network (Figure S1; Table S5). Among these 51 annotations, seven candidate structures were identical (Figure S2), and one of them at m/z 566.2516 ($[M+H]^+$ $C_{32}H_{38}O_9$) was dereplicated by MarinLit as godavarin K,

3.5 Antimicrobial and cytotoxic activities

None of the 23 cyanobacterial extracts tested against four pathogenic bacterial strains (*S. aureus* ATCC 25923, *E. coli* ATCC 25922, *P. aeruginosa* PAO1, and *E. faecalis* ATCC29212) displayed any significant antimicrobial activity, with minimum inhibitory concentration (MIC) values $> 200 \mu\text{g. mL}^{-1}$ (Text S1). Of all 23 strains tested against the Chinese hamster ovary (CHO) cells, only PMC 1121.19, *Capilliphycus* sp. showed cytotoxic activity with a 50% inhibitory concentration (IC_{50}) value of $15.73 \pm 1.64 \mu\text{g. mL}^{-1}$. In addition, weak cytotoxic activity was also observed with both *Hydrocoleum* sp. Strains PMC 1103.19 and PMC 1116.19, with IC_{50} values of $94.54 \pm 3.98 \mu\text{g. mL}^{-1}$ and $86.37 \pm 4.16 \mu\text{g. mL}^{-1}$, respectively (Figure 8A).

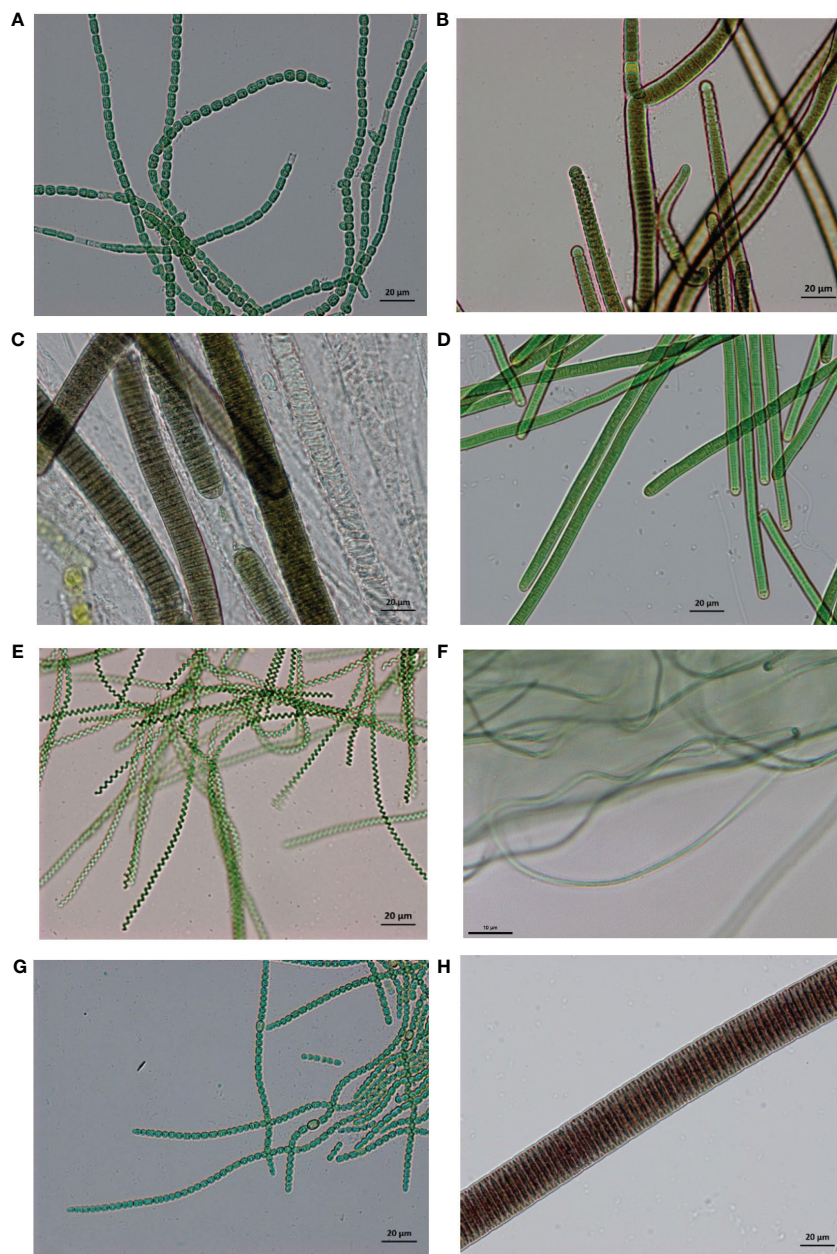


FIGURE 6

Cyanobacterial strains. (A) PMC 1097.19 (*Hapalosiphon welwitschii*) (B) PMC 1101.19 (*Brasilonema* sp.); (C) PMC 1108.19 (*Dapis* sp.); (D) PMC 1121.19 (*Capilliphycus* sp.); (E) PMC 1141.19 (*Spirulina* sp. 2); (F) PMC 1124.19 (*Gen. Nov. 1* sp.); (G) PMC 1136.19 (*Wollea* sp. 1); (H) PMC 1116.19 (*Hydrocoleum* sp.).

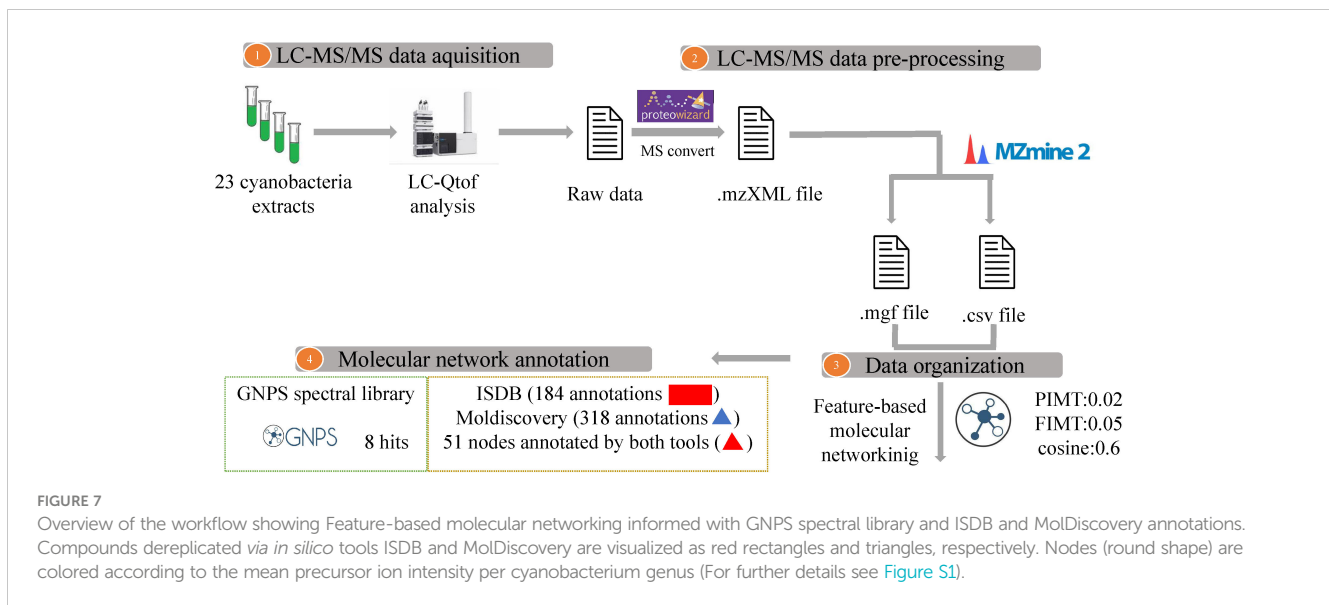
3.6 Anthelmintic activities

All 23 cyanobacteria extracts showed at least some degree of anthelmintic activity based on the reduced mobility of the *Litomosoides sigmodontis* microfilaria (Figure 8B). In particular, extracts from *Capilliphycus* sp. (PMC 1121.19) and *Thainema* sp. 1 (PMC 1125.19) completely inhibited their movements, with mobility scores down to 0 (no mobility). Extracts from *Hydrocoleum* sp. (PMC 1116.19), *Wollea* sp. (1138.19), *Planktothrix mougeoti* (1100.19), *Thainema* sp. 2 (1126.19), and

Hapalosiphon welwitschii (1099.19) resulted in reducing microfilaria activity (< 0.5), meaning that microfilaria showed very limited mobility when exposed.

3.7 Antibiofilm activities

The antibiofilm activity of the 23 crude extracts was measured using the percentage of inhibition biofilm formation of the bacterial strain *Pseudomonas aeruginosa* MUC-N1. A majority of the



cyanobacterial strains had low antibiofilm activity against this strain ranging from 2 to 30%. Three strains, namely PMC 1119.19, 1121.19 (*Capilliphycus* sp.), and PMC 1116.19 (*Hydrocoleum* sp.), showed moderate antibiofilm activity around 42% (Figure 8C). Three strains corresponding to two known species, namely PMC 1097.19, 1099.19 (*Hapalosiphon welwitschii*), and PMC 1100.19 (*Planktothrix mougeotii*) displayed the highest antibiofilm activities, ranging from 58.9 to 62.4%. In contrast, six other strains PMC 1101.19 (*Brasilonema* sp.), 1125.19, 1126.19 (*Thainema* sp. 1 and 2), 1127.19 (*Capilliphycus* sp.), as well as 1136.19, 1138.19 (*Wollea* sp. 1 and 2), showed negative inhibition, particularly strain 1125.19 (*Thainema* sp. 1, 153.7%) indicating that exposure increased biofilm growth compared to control. Other strains did not show clear-cut inhibition or promotion of biofilm formation.

4 Discussion

4.1 Biofilms in Mayotte display diverse compositions, and diverse cyanobacteria

Identifying cyanobacteria-containing biofilms in the field is not always straightforward. In this study, we sampled biofilms displaying different shades of green, as well as some brownish, slimy, or crustose biofilms. They mostly occurred on sediment surfaces and tree bark, and some of them, for example sample S21, covered very large areas. Despite a tendency for some of the greener ones to display higher relative abundances of cyanobacteria, the abundances were highly variable, pointing out the heterogeneity in biofilm composition. Furthermore, no single cyanobacterial ASVs occurred in more than five out of the 27 biofilm samples, confirming that different biofilms contain different cyanobacteria. Overall, this indicates that each type of biofilm is a potential source of novel strains of cyanobacteria and should be considered for a proper description of the benthic biofilm-forming cyanobacterial diversity.

4.2 Isolation of some of the most abundant cyanobacteria present in biofilms

The 43 strains isolated in this study represent 22 species-level taxa based on a 98.65% similarity threshold over the full-length 16S rRNA-encoding gene. Interestingly, 13 of the isolated species-level taxa were also identified during the characterization of biofilm composition using 16S rRNA metabarcoding. They represent only 8.9% of all identified cyanobacterial ASVs, suggesting that only a minor fraction of the actual diversity of cyanobacteria has been successfully isolated. This is consistent with the acknowledged fact that microbiologists tend to isolate only a small subset of the actual diversity present in Nature (Staley et al., 1985). However, if we consider only the most abundant cyanobacteria that occur in biofilms, the picture is slightly more encouraging. In fact, only 15 cyanobacterial ASVs represented more than 5% of the total 16S rRNA reads in at least one biofilm sample, while none of the other 142 ever represented more than 5% of the total reads in any biofilm sample. Focusing on filamentous morphotypes, we successfully isolated seven of these 15 most abundant cyanobacteria (47%), suggesting that isolating a significant fraction of the most abundant cyanobacterial members of benthic biofilms is tractable, and that continued isolation effort would likely yield additional taxa of ecological importance given their abundance.

Although various studies have successfully reported the isolation of cyanobacterial strains from mangroves (Cecccon et al., 2019; Wu et al., 2022; Zhang et al., 2022), these are usually not associated with a characterization of the communities from which they were isolated, and consequently, the authors are usually unable to address whether they have isolated any of the actual abundant ones. On the other hand, our results suggest that standard isolation procedures can already yield some of the abundant biofilm-associated cyanobacteria, as well as rarer members of the community. Examples of the latter likely include the nine species that we isolated as strains but never detected in biofilm 16S rRNA datasets, in line with the claim that lab-based isolation procedures

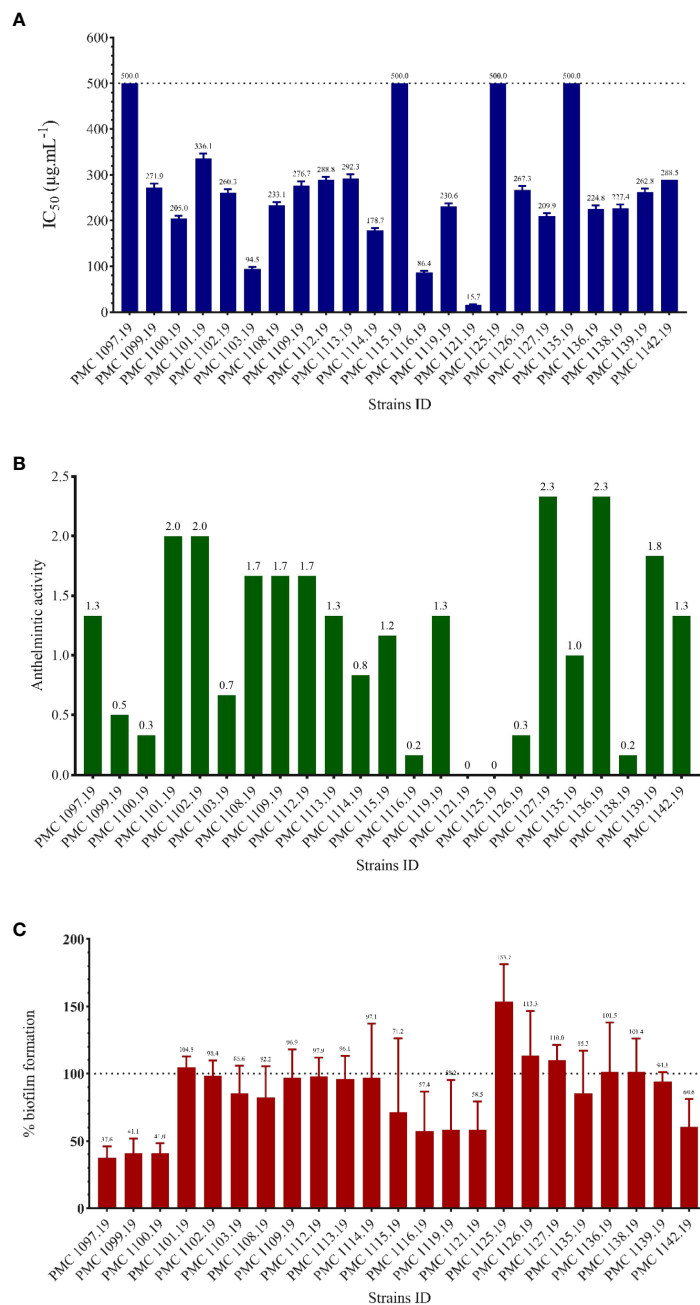


FIGURE 8 Summary of the evaluation of activities of the 23 cyanobacterial strains. (A): activity against CHO cells; (B): activity against filarial nematodes (qualitative assay); (C): antibiofilm activity.

also often yield rare bacteria (Ferris and Hirsch, 1991), as the culture media compositions or culture conditions are very different from that of natural environment. These rare bacteria may have been detected provided greater depth of sequencing. Isolating, cultivating, and maintaining the abundant members of biofilms in publicly available collections such as the PMC collection provides unique opportunities to unravel biofilm functioning and ecology (Liu et al., 2016; Tamminen et al., 2022), as well as their potential to produce new molecules, and preserve a snapshot of the ecologically important microbial diversity (Delgado-Baquerizo et al., 2016; Vitorino and Bessa, 2018; Gebbie et al., 2020). *In situ* abundance

could even become a criterion to select which strains should be maintained in culture collections.

4.3 Mangroves of Mayotte island are a source of novel cyanobacteria

This study showed that only nine out of 43 strains can be assigned to a described species based on 16S rRNA comparative analysis, representing three species. The other 34 isolated cyanobacterial strains could not be assigned to a species, and

belong to 19 species-level taxa for which no name could be proposed (Komárek et al., 2014). Based on current similarity criteria, five of the strains would even warrant classification in three new genera. High levels of novelty distributed over several orders of Cyanobacteria were recently reported in several mangrove habitats, for example in Guadeloupe island (Lesser Antilles), including strains within the Oscillatoriales, Synechococcales, and Nostocales (Duperron et al., 2020). Interestingly, some of the strains isolated in Mayotte have very closely related conspecifics in very distant locations. Strains corresponding to *Thainema* sp. 2 from this study (PMC 1126.19) were found abundant in the mangroves of Cananéia municipality (25°05′02″ S, 47°57′42″ W) and the city of Bertioga (23°53′49″ S, 46°12′28″ W), Brazil (Silva et al., 2014), despite being separated by the entire Atlantic Ocean and the African continent. This illustrates that some of the species could be widely distributed. Synechococcales diversity was limited in our study, while this order was for example found abundant in the Mooriganga Estuary, India (Bhadury and Singh, 2020). Differences in environmental factors including anthropogenic impacts as well as isolation bias (we focused on filamentous species) may have led to this result (Rigonato et al., 2012). Similarly, the strains in the *Phormidium* and *Oscillatoria* genera were present in 25% and 20% of mangrove forest samples in the Persian Gulf (Zaheri et al., 2021), while no species within these two genera was found in our study. These examples shown here illustrate that there also exist potential differences linked to geography.

Further features beyond simple 16S rRNA dissimilarity- and phylogeny-based criteria are required for determining the accurate status of strains as new genera or species. Polyphasic methods will be necessary to provide a proper taxonomic description, which are beyond the scope of this paper (Komárek et al., 2014; Cellamare et al., 2018). Nevertheless, the high level of taxonomic novelty found in the coastal mangrove biofilms in Mayotte is already self-evident

based on our results. Very limited data are available on the taxonomic diversity of marine cyanobacteria in Mayotte, except for a recent paper describing Nostocales cyanobacterial strains, which are not closely related to the strains described herein, and belong to the genera *Chrysochlorum*, *Dolichospermum*, *Raphidiopsis* (Duval et al., 2018). Overall, the novelty level shown here shows that the cyanobacterial diversity is mostly unexplored in Mayotte. The potential of tropical ecosystems, particularly mangroves, as reservoirs of cyanobacterial diversity (Aburto-Oropeza et al., 2008; Liao et al., 2020; Roberts et al., 2021), as well as the predominance of orders Oscillatoriales and Synechococcales among the recovered strains (Zubia et al., 2016; Zubia et al., 2019), have been highlighted by several authors.

4.4 The benthic cyanobacterial strains reveal a high level of chemical novelty

The annotation of 2,667 nodes organized into 131 clusters at the genus identification level revealed that many were strain-specific or taxa-specific, suggesting important inter-strain heterogeneity in their produced molecules. The limited coverage of cyanobacteria in existing databases only allowed us reliable annotation of very few compounds.

Among the ISDB-DNP annotated nodes, 28 were from the marine field, 15 from cyanobacteria, and 6 compounds from bacteria. For a deeper analysis, the results generated from different *in silico* annotation tools, namely ISDB, MolDiscovery, and SIRIUS in conjunction with the marine natural product database MarinLit were combined. The three databases (MarinLit, ISDB, and MolDiscovery) consensually proposed godavarin K as the most probable annotated compound for $[M+H]^+$ ion m/z 567.26008 (Text S2). Interestingly, SIRIUS did not suggest godavarin K as a structure candidate. Further exploration of the

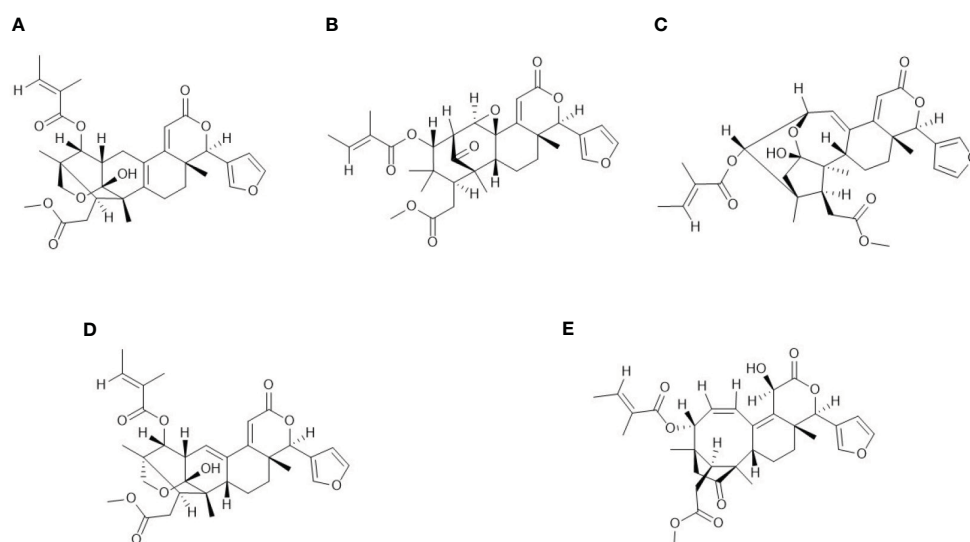


FIGURE 9

Structures of the five 5 isomers annotated for the node at $[M+H]^+$ ion m/z 567.26008: (A) Godavarin K; (B) Granatumin C; (C) Andhraxylocarpins A; (D) Krishnagranatins B; (E) Thaigranatin R.

database PubChem (Kim, 2021) revealed that the molecular formula $C_{29}H_{36}O_9$ (molecular weight $528.6 \text{ g}\cdot\text{mol}^{-1}$) was erroneously attributed to godavarin K. Moreover, it turns out that this entry in PubChem was linked to the reference of godavarin A-J (Li et al., 2010), which does not include godavarin K.

In this study, the node annotated as godavarin K was previously isolated from seeds of mangrove tree *Xylocarpus moluccensis*, that were collected in the wetlands of Godavari estuary, Andhra Pradesh, India (Li et al., 2011). In addition to godavarin K, dereplication of the molecular formula $C_{32}H_{38}O_9$ against MarinLit resulted in four limonoids including granatumin C (Li et al., 2009), krishnagranatin B (Liu et al., 2018), thaigranatin R (Ren et al., 2021), and andraxylcarpin A (Li et al., 2012). All of them were obtained from seeds of mangrove trees *X. moluccensis* or *X. granatum*, or both. Furthermore, the *in silico* annotation tool SIRIUS proposed only granatumin C, as a candidate structure.

In addition, five isomers (Figure 9) were shown after a filter of the formula $C_{32}H_{38}O_9$ in MarinLit was applied, and all five isomeric compounds were isolated from the seeds of the mangrove trees *Xylocarpus moluccensis* or *Xylocarpus granatum* or both, collected from wetlands in India or Thailand and published by the same team (Li, 2009; Li et al., 2011; Li et al., 2012; Liu et al., 2018; Ren et al., 2021). Our new results suggest that the five isomer compounds might have been produced by seed-associated cyanobacteria that may be associated with the mangrove trees. Whatsoever, organism-associated cyanobacteria must be considered as potential producers of some molecules that are usually attributed to their hosts (Habibi et al., 2017), as shown in a recent example in which cyanobacteria were the probable source of a molecule found associated with a marine sponge (Castaldi et al., 2022).

Interestingly, the node annotated as godavarin K was only found in strain *Planktothrix mougeotii*, PMC 1114.19, isolated from sample S21 collected in the Dembeni mangrove. Of note, four additional strains isolated from the same source were also identified as *P. mougeotii* but did not display the node annotated as godavarin K. This may be due to chemical heterogeneity between individuals, possibly underpinned by genome variability between strains as previously highlighted in several studies on *Microcystis* and *Aphanizomenon* (Meyer et al., 2017a; Pérez-Carrascal et al., 2019).

4.5 Biological activities as assets in the ecology of the benthic cyanobacteria from Mayotte?

No antimicrobial activity and limited cytotoxic activity on the cell lineages tested were detected for the 23 tested strains. On the other hand, some of these strains showed significant anthelmintic and antibiofilm activities and will be further explored to identify and characterize specific molecules responsible for these activities. Strains of *Planktothrix mougeotii*, for example, PMC 1100.19, displayed very high anti-biofilm activity in our lab-based test. In nature, antibiofilm activity could be relevant to the biofilm lifestyle by preventing overgrowth by competing microorganisms. Although actual *in situ* relevance of the activity measured in our test remains

to be evaluated, *P. mougeotii* represents 94.5% of cyanobacteria and 44% of all bacteria in sample S21, suggesting it can outcompete other strains present. Similarly, our tests demonstrated anthelmintic activity in several strains. Nematode worms include various species that can graze on biofilms (Moon et al., 2021). Despite that our tests were targeted towards health-relevant nematodes, this type of strong anthelmintic activity could provide a level of protection against grazing. Certain species such as *Hydrocoleum* sp., which makes up 20% of cyanobacteria in a biofilm, displayed both types of activities. Indeed, one strain inhibits biofilm formation (PMC 1116.19) while another is efficient against nematodes (PMC 1103.19). *Wollea* sp. 2 (PMC 1138.10, 1140.19) represented 28% of cyanobacteria and 16% of all bacteria in one biofilm and also showed anthelmintic activity. However, opposite results were also observed with several strains displaying biofilm growth-promoting activity culminating in strain PMC 1125.19 (*Thainema* sp. 1). Biofilm growth inhibition is thus not systematic.

Activities observed in the different strains indicate that not all strains within a given cyanobacterial genus or species express the same activities, even when cultured under the same conditions. It suggests that specific genes or metabolic pathways may be present or expressed in some but not all strains of a given taxon, resulting in inter-strain heterogeneity that could be related to gene exchanges (e.g. lateral transfers). It also points towards the possibility that some of the activities are the result of interactions with members of the phycosphere, consisting of other microorganisms (mainly bacteria) that are isolated from the cyanobacteria and co-cultured with them (Zhu et al., 2016). This phycosphere interacts with and influences the physiology of the cyanobacterial strains, as has been seen in other organisms that coexist with microbiota, and may even be in an obligate symbiotic relationship. Investigating inter-strains genomic and phycosphere variability will be necessary to understand why different strains within a single species and cultivated under comparable conditions might demonstrate significantly distinct chemical compounds and activities.

5 Conclusions

This study confirms that mangrove biofilms harbor a largely untapped diversity of novel cyanobacteria. A significant proportion of the abundant species can be isolated using reasonably simple methods. Benthic mangrove cyanobacteria produce a wide diversity of metabolites, of which little is known. They may include compounds that are commonly attributed to other organisms, but which may in fact be produced by organism-associated cyanobacteria, which need to be considered as potential producers of molecules usually attributed to their hosts. Although no antimicrobial activities against common pathogens were detected, we cannot exclude that it may be due to the chosen extraction method, and other types of extractions should be tested. Other activities such as anthelmintic and antibiofilm activities were frequently observed. The molecules and genetic basis responsible for these activities should be further explored, and whether activities measured in a laboratory setting are relevant to cyanobacteria-containing biofilms chemical ecology *in situ* needs to be tested.

They could contribute to the fitness of biofilm-forming cyanobacteria in mangrove habitats and warrant further study to investigate their potential uses and to understand the chemical ecology of mangrove ecosystems.

Supplementary data to this article can be found online at: (HTTP address).

Data availability statement

The datasets presented in this study can be found in online repositories. The names of the repository/repositories and accession number(s) can be found in the article/**Supplementary Material**.

Author contributions

Conceptualization: SD, M-LB-K. Field work: SD, CB, MT, CG. Lab work and data curation: HW, SD, CD, CB, MB, J-MB, AC, FC, CM. Statistical analyses: HW, SH, M-LB-K. Funding acquisition and Project supervision: SD, M-LB-K. Original draft: HW, MLBK, SD. Review and editing: all authors.

Funding

We acknowledge the financial support of the CNRS MITI X-Life 2018-2019 program (CABMAN project), the ATM CHEMCYANGROV from the 2019 MNHN grant “biodiversity of

microorganisms”, for funding lab and fieldwork, and HBC (Huazhi Biotechnology Co., Ltd) which provided scholarship to HW. The authors declare that this study received funding from HBC (Huazhi Biotechnology Co., Ltd). The funder was not involved in the study design, collection, analysis, interpretation of data, the writing of this article or the decision to submit it for publication.

Conflict of interest

The authors declare that the research was conducted in the absence of any commercial or financial relationships that could be construed as a potential conflict of interest.

Publisher’s note

All claims expressed in this article are solely those of the authors and do not necessarily represent those of their affiliated organizations, or those of the publisher, the editors and the reviewers. Any product that may be evaluated in this article, or claim that may be made by its manufacturer, is not guaranteed or endorsed by the publisher.

Supplementary material

The Supplementary Material for this article can be found online at: <https://www.frontiersin.org/articles/10.3389/fmars.2023.1201594/full#supplementary-material>

References

- Aburto-Oropeza, O., Ezcurra, E., Danemann, G., Valdez, V., Murray, J., and Sala, E. (2008). Mangroves in the gulf of California increase fishery yields. *Proc. Natl. Acad. Sci. USA* 105, 10456–10459. doi: 10.1073/pnas.0804601105
- Adame, M. F., Teutli, C., Santini, N. S., Caamal, J. P., Zaldivar-Jiménez, A., Hernández, R., et al. (2014). Root biomass and production of mangroves surrounding a karstic oligotrophic coastal lagoon. *Wetlands* 34, 479–488. doi: 10.1007/s13157-014-0514-5
- Allard, P. M., Péresse, T., Bisson, J., Gindro, K., Marcourt, L., Pham, V. C., et al. (2016). Integration of molecular networking and *in-silico* MS/MS fragmentation for natural products dereplication. *Anal. Chem.* 88, 3317–3323. doi: 10.1021/acs.analchem.5b04804
- Alvarenga, D. O., Rigonato, J., Branco, L. H. Z., and Fiore, M. F. (2015). Cyanobacteria in mangrove ecosystems. *Biodivers. Conserv.* 24, 799–817. doi: 10.1007/s10531-015-0871-2
- Amir, A., Daniel, M., Navas-Molina, J., Kopylova, E., Morton, J., Xu, Z. Z., et al. (2017). Deblur rapidly resolves single-. *Am. Soc. Microbiol.* 2, 1–7. doi: 10.1128/mSystems.00191-16
- Ammar, M., Comte, K., Chi, T., Du, T., and El Bour, M. (2014). Initial growth phases of two bloom-forming cyanobacteria (*Cylindrospermopsis raciborskii* and *Planktothrix agardhii*) in monocultures and mixed cultures depending on light and nutrient conditions. *Ann. Limnol.* 50, 231–240. doi: 10.1051/limn/2014096
- Berthold, D. E., Lefler, F. W., and Laughinghouse, H. D. (2021). Untangling filamentous marine cyanobacterial diversity from the coast of South Florida with the description of Vermifilaceae fam. nov. and three new genera: *Leptochromothrix* gen. nov., *Ophiophycus* gen. nov., and *Vermifilum* gen. nov. *Mol. Phylogenet. Evol.* 160, 107010. doi: 10.1016/j.ympev.2020.107010
- Bhadury, P., and Singh, T. (2020). Analysis of marine planktonic cyanobacterial assemblages from mooriganga estuary, Indian sundarbans using molecular approaches. *Front. Mar. Sci.* 7. doi: 10.3389/fmars.2020.00222
- Bich-Loan, N. T., Kien, K. T., Thanh, N. L., Kim-Thanh, N. T., Huy, N. Q., The-Hai, P., et al. (2021). Toxicity and anti-proliferative properties of anisomeles indica ethanol extract on cervical cancer hela cells and Zebrafish embryos. *Life* 11 (3), 1–15. doi: 10.3390/life11030257
- Blasco, F., Saenger, P., and Janodet, E. (1996). Mangroves as indicators of coastal change. *Catena* 27, 167–178. doi: 10.1016/0341-8162(96)00013-6
- Boukerb, A. M., Simon, M., Pernet, E., Jouault, A., Portier, E., and Persyn, E. (2020). Draft genome sequences of four *Pseudomonas aeruginosa*. *Microbiol. Resour. Announc.* 3, 1–3. doi: 10.1128/mra.01286-19
- Bulsecq, A. N., Zengler, K., and Diego, S. (2020). Applied and environmental science crossm introducing the mangrove microbiome initiative: identifying microbial research priorities and approaches to better. *Appl. Environ. Sci.* 5, 1–9.
- Busi, S. B., Bourquin, M., Fodelianakis, S., Michoud, G., Kohler, T. J., Peter, H., et al. (2022). Genomic and metabolic adaptations of biofilms to ecological windows of opportunity in glacier-fed streams. *Nat. Commun.* 13, 1–15. doi: 10.1038/s41467-022-29914-0
- Caires, T. A., de Mattos Lyra, G., Hentschke, G. S., de Gusmão Pedrini, A., Sant’Anna, C. L., and de Castro Nunes, J. M. (2018a). *Neolyngbya* gen. nov. (Cyanobacteria, Oscillatoriaceae): a new filamentous benthic marine taxon widely distributed along the Brazilian coast. *Mol. Phylogenet. Evol.* 120, 196–211. doi: 10.1016/j.ympev.2017.12.009
- Caires, T. A., Lyra, G., de, M., Hentschke, G. S., da Silva, A. M. S., de Araújo, V. L., et al. (2018b). Polyphasic delimitation of a filamentous marine genus, *capillus* gen. nov. (cyanobacteria, oscillatoriaceae) with the description of two Brazilian species. *Algae* 33, 291–304. doi: 10.4490/algae.2018.33.11.25
- Cao, L., Guler, M., Tagirdzhanov, A., Lee, Y. Y., Gurevich, A., and Mohimani, H. (2021). MolDiscovery: learning mass spectrometry fragmentation of small molecules. *Nat. Commun.* 12, 1–13. doi: 10.1038/s41467-021-23986-0
- Castaldi, A., Teta, R., Esposito, G., Beniddir, M. A., De Voogd, N. J., Duperron, S., et al. (2022). Computational metabolomics tools reveal subarmigerides, unprecedented linear peptides from the marine sponge holobiont *Callyspongia subarmigera*. *Mar. Drugs* 20, 1–13. doi: 10.3390/md20110673

- Ceccon, D. M., Faoro, H., Lana, P., da, C., de Souza, E. M., and de Pedrosa, F. O. (2019). Metataxonomic and metagenomic analysis of mangrove microbiomes reveals community patterns driven by salinity and pH gradients in Paranaguá Bay, Brazil. *Sci. Total Environ.* 694, 133609. doi: 10.1016/j.scitotenv.2019.133609
- Cellamare, M., Duval, C., Drelin, Y., Djediat, C., Touibi, N., Agogue, H., et al. (2018). Characterization of phototrophic microorganisms and description of new cyanobacteria isolated from the saline-alkaline crater-lake Dziani Dzaha (Mayotte, Indian Ocean). *FEMS Microbiol. Ecol.* 94, 1–25. doi: 10.1093/FEMSEC/FIY108
- Coffey, B. M., and Anderson, G. G. (2014). Biofilm formation in the 96-well microtiter plate. *Methods Mol. Biol.* 1149, 631–641. doi: 10.1007/978-1-4939-0473-0_48
- Cole, J. R., Wang, Q., Cardenas, E., Fish, J., Chai, B., Farris, R. J., et al. (2009). The ribosomal database project: improved alignments and new tools for rRNA analysis. *Nucleic Acids Res.* 37, 141–145. doi: 10.1093/nar/gkn879
- Delgado-Baquerizo, M., Maestre, F. T., Reich, P. B., Jeffries, T. C., Gaitan, J. J., Encinar, D., et al. (2016). Microbial diversity drives multifunctionality in terrestrial ecosystems. *Nat. Commun.* 7, 1–8. doi: 10.1038/ncomms10541
- Demay, J., Bernard, C., Reinhardt, A., and Marie, B. (2019). Natural products from cyanobacteria: focus on beneficial activities. *Mar. Drugs* 17, 1–49. doi: 10.3390/md17060320
- Doncheva, N. T., Morris, J. H., Gorodkin, J., and Jensen, L. J. (2019). Cytoscape StringApp: network analysis and visualization of proteomics data. *J. Proteome Res.* 18, 623–632. doi: 10.1021/acs.jproteome.8b00702
- Du, X., Smirnov, A., Pluskal, T., Jia, W., and Sumner, S. (2020). Metabolomics data preprocessing using ADAP and MZmine 2. *Methods Mol. Biol.* 2104, 25–48. doi: 10.1007/978-1-0716-0239-3_3
- Dührkop, K., Shen, H., Meusel, M., Rousu, J., and Böcker, S. (2015). Searching molecular structure databases with tandem mass spectra using CSI: FingerID. *Proc. Natl. Acad. Sci. U. S. A.* 112, 12580–12585. doi: 10.1073/pnas.1509788112
- Duperron, S., Beniddir, M. A., Durand, S., Longeon, A., Duval, C., Gros, O., et al. (2020). New benthic cyanobacteria from gadeloupe mangroves as producers of antimicrobials. *Mar. Drugs* 18, 1–14. doi: 10.3390/md18010016
- Duval, C., Thomazeau, S., Drelin, Y., Yéprémian, C., Bouvy, M., Couloux, A., et al. (2018). Phylogeny and salt-tolerance of freshwater Nostocales strains: contribution to their systematics and evolution. *Harmful Algae* 73, 58–71. doi: 10.1016/j.hal.2018.01.008
- Edgar, R. C., Haas, B. J., Clemente, J. C., Quince, C., and Knight, R. (2011). UCHIME improves sensitivity and speed of chimera detection. *Bioinformatics* 27, 2194–2200. doi: 10.1093/bioinformatics/btr381
- Ferris, M. J., and Hirsch, C. F. (1991). Method for isolation and purification of cyanobacteria. *Appl. Environ. Microbiol.* 57, 1448–1452. doi: 10.1128/aem.57.5.1448-1452.1991
- Fadeev, E., Cardozo-Mino, M. G., Rapp, J. Z., Bienhold, C., Salter, I., Salman-Carvalho, V., et al. (2021). Comparison of Two 16S rRNA Primers (V3–V4 and V4–V5) for Studies of Arctic Microbial Communities. *Front. Microbiol.* 12, 1–11. doi: 10.3389/fmicb.2021.637526
- Gebbie, L., Dam, T. T., Ainscough, R., Palfreyman, R., Cao, L., Harrison, M., et al. (2020). A snapshot of microbial diversity and function in an undisturbed sugarcane bagasse pile. *BMC Biotechnol.* 20, 1–17. doi: 10.1186/s12896-020-00609-y
- Gugger, M., Lyra, C., Henriksen, P., Couté, A., Humbert, J. F., and Sivonen, K. (2002). Phylogenetic comparison of the cyanobacterial genera *Anabaena* and *Aphanizomenon*. *Int. J. Syst. Evol. Microbiol.* 52, 1867–1880. doi: 10.1099/ijso.0.02270-0
- Habibi, A., Zayadan, B. K., Baizhigitova, A., Alemyar, S., and Bauyenova, M. O. (2017). The effect of isolated cyanobacteria on rice seed germination and growth. *Eurasian J. Ecol.* 2, 114–122. doi: 10.26577/eje-2017-2-772
- Hall, M. W., and Beiko, R. G. (2018). 16S rRNA Gene Analysis with QIIME2. *Methods Mol. Biol.* 1849, 113–129. doi: 10.1007/978-1-4939-8728-3_8
- Hamlaoui, S., YéPRÉMIAN, C., Duval, C., Marie, B., DjéDIAT, C., Piquet, B., et al. (2022). The culture collection of cyanobacteria and microalgae at the French national museum of natural history: a century old but still alive and kicking! including in memoriam: professor Alain Couté. *Cryptogam. Algal.* 43, 41–83. doi: 10.5252/cryptogamie-algologie2022v43a3
- Hawryluk, N., Zhiru, L., Carlow, C., Gokool, S., Townson, S., Kreiss, T., et al. (2022). Filarial nematode phenotypic screening cascade to identify compounds with anti-parasitic activity for drug discovery optimization. *Int. J. Parasitol. Drugs Drug Resist.* 19, 89–97. doi: 10.1016/j.ijpddr.2022.06.002
- Kim, S. (2021). Exploring chemical information in pubchem. *Curr. Protoc.* 1, e217. doi: 10.1002/cpz1.217
- Kim, M., Oh, H. S., Park, S. C., and Chun, J. (2014). Towards a taxonomic coherence between average nucleotide identity and 16S rRNA gene sequence similarity for species demarcation of prokaryotes. *Int. J. Syst. Evol. Microbiol.* 64, 346–351. doi: 10.1099/ijso.0.059774-0
- Komárek, J., Kaštovský, J., Mareš, J., and Johansen, J. R. (2014). Taxonomic classification of cyanoprokaryotes (cyanobacterial genera) 2014, using a polyphasic approach. *Preslia* 86, 295–335.
- Kozliková-Zapomělová, E., Chatchawan, T., Kaštovský, J., and Komárek, J. (2016). Phylogenetic and taxonomic position of the genus *Wolleea* with the description of *Wolleea salina* sp. nov. (Cyanobacteria, Nostocales). *Fottea* 16, 43–55. doi: 10.5507/fot.2015.026
- Li, M.-Y. (2009). Granatamins A-G, limonoids from the seeds of a *Krishna Mangrove*, *Xylocarpus granatum* Min-Yi. *J. Nat. Prod.* 72, 2110–2114. doi: 10.1002/cbdv.201200021
- Li, J., Li, M. Y., Bruhn, T., Götz, D. C. G., Xiao, Q., Satyanandamurty, T., et al. (2012). Andhraxylocarpins A-E: structurally intriguing limonoids from the true mangroves *xylocarpus granatum* and *xylocarpus moluccensis*. *Chem. A. Eur. J.* 18, 14342–14351. doi: 10.1002/chem.201202356
- Li, J., Li, M. Y., Feng, G., Xiao, Q., Sinkkonen, J., Satyanandamurty, T., et al. (2010). Limonoids from the seeds of a Godavari mangrove, *Xylocarpus moluccensis*. *Phytochemistry* 71, 1917–1924. doi: 10.1016/j.phytochem.2010.07.015
- Li, J., Li, M. Y., Satyanandamurty, T., and Wu, J. (2011). Godavarin K: a new limonoid with an oxygen bridge between C(1) and C(29) from the godavari mangrove *Xylocarpus moluccensis*. *Helv. Chim. Acta* 94, 1651–1656. doi: 10.1002/hlca.201100022
- Li, M.-Y., Yang, X.-B., Pan, J.-Y., Feng, G., Xiao, Q., Sinkkonen, J., et al. (2009). Granatamins A–G, limonoids from the seeds of a *Krishna Mangrove*, *Xylocarpus granatum*. *J. Nat. Prod.* 72, 2110–2114. doi: 10.1021/np900625w
- Liao, S., Wang, Y., Liu, H., Fan, G., Sahu, S. K., Jin, T., et al. (2020). Deciphering the microbial taxonomy and functionality of two diverse mangrove ecosystems and their potential abilities to produce bioactive compounds. *mSystems* 5, 1–19. doi: 10.1128/msystems.00851-19
- Liu, R. X., Liao, Q., Shen, L., and Wu, J. (2018). *Krishnagranatins A–I*: new limonoids from the mangrove, *Xylocarpus granatum*, and NF- κ B inhibitory activity. *Fitoterapia* 131, 96–104. doi: 10.1016/j.fitote.2018.08.011
- Liu, W., Røder, H. L., Madsen, J. S., Bjarnsholt, T., Sørensen, S. J., and Burmølle, M. (2016). Interspecific bacterial interactions are reflected in multispecies biofilm spatial organization. *Front. Microbiol.* 7. doi: 10.3389/fmicb.2016.01366
- Ludwig, W. (2007). Nucleic acid techniques in bacterial systematics and identification. *Int. J. Food Microbiol.* 120, 225–236. doi: 10.1016/j.ijfoodmicro.2007.06.023
- Meyer, N., Bigalke, A., Kaulfuß, A., and Pohnert, G. (2017b). Strategies and ecological roles of algicidal bacteria. *FEMS Microbiol. Rev.* 41, 880–899. doi: 10.1093/femsr/fux029
- Meyer, K. A., Davis, T. W., Watson, S. B., Deneff, V. J., Berry, M. A., and Dick, G. J. (2017a). Genome sequences of lower great lakes *Microcystis* sp. reveal strain-specific genes that are present and expressed in western Lake Erie blooms. *PLoS One* 12, 1–21. doi: 10.1371/journal.pone.0183859
- Moon, C. D., Carvalho, L., Kirk, M. R., McCulloch, A. F., Kittelmann, S., Young, W., et al. (2021). Effects of long-acting, broad spectra anthelmintic treatments on the rumen microbial community compositions of grazing sheep. *Sci. Rep.* 11, 1–14. doi: 10.1038/s41598-021-82815-y
- Mühr, L. S. A., Lagheden, C., Hassan, S. S., Kleppe, S. N., Hultin, E., and Dillner, J. (2020). *De novo* sequence assembly requires bioinformatic checking of chimeric sequences. *PLoS One* 15, 1–11. doi: 10.1371/journal.pone.0237455
- Myers, O. D., Sumner, S. J., Li, S., Barnes, S., and Du, X. (2017). One step forward for reducing false positive and false negative compound identifications from mass spectrometry metabolomics data: new algorithms for constructing extracted ion chromatograms and detecting chromatographic peaks. *Anal. Chem.* 89, 8696–8703. doi: 10.1021/acs.analchem.7b00947
- Nellemann, C., Corcoran, E., Duarte, C. M., Valdés, L., De Young, C., Fonseca, L., et al. (2009) *Blue carbon: A Rapid Response Assessment*. Available at: http://www.grida.no/files/publications/blue-carbon/BlueCarbon_screen.pdf.
- Newman, L., Duffus, A. L. J., and Lee, C. (2016). Using the free program MEGA to build phylogenetic trees from molecular data. *Am. Biol. Teach.* 78, 608–612. doi: 10.1525/abt.2016.78.7.608
- Nothias, L. F., Petras, D., Schmid, R., Dührkop, K., Rainer, J., Sarvepalli, A., et al. (2020). Feature-based molecular networking in the GNPS analysis environment. *Nat. Methods* 17, 905–908. doi: 10.1038/s41592-020-0933-6
- Pérez-Carrascal, O. M., Terrat, Y., Giani, A., Fortin, N., Greer, C. W., Tromas, N., et al. (2019). Coherence of *microcystis* species revealed through population genomics. *ISME J.* 13, 2887–2900. doi: 10.1038/s41396-019-0481-1
- Petrescu, F. I. T., and Ungureanu, L. M. (2022). About the cyanobacteria and stromatolites. *Online J. Biol. Sci.* 22, 87–111. doi: 10.3844/ojbsci.2022.87.111
- Pluskal, T., Castillo, S., Villar-Briones, A., and Orešič, M. (2010). MZmine 2: modular framework for processing, visualizing, and analyzing mass spectrometry-based molecular profile data. *BMC Bioinf.* 11, 1–11. doi: 10.1186/1471-2105-11-395
- Posada, D., and Buckley, T. R. (2004). Model selection and model averaging in phylogenetics: advantages of akaike information criterion and bayesian approaches over likelihood ratio tests. *Syst. Biol.* 53, 793–808. doi: 10.1080/10635150490522304
- Reef, R., Feller, I. C., and Lovelock, C. E. (2010). Nutrition of mangroves. *Tree Physiol.* 30, 1148–1160. doi: 10.1093/treephys/tpq048
- Ren, Y. X., Zou, X. P., Li, W. S., Wu, J., and Shen, L. (2021). Discovery of Thai mangrove tetranortriterpenoids as agonists of human pregnane-X-receptor and inhibitors against human carboxylesterase 2. *Bioorg. Chem.* 107, 104599. doi: 10.1016/j.bioorg.2020.104599
- Rigonato, J., Alvarenga, D. O., Andreote, F. D., Dias, A. C. F., Melo, I. S., Kent, A., et al. (2012). Cyanobacterial diversity in the phyllosphere of a mangrove forest. *FEMS Microbiol. Ecol.* 80, 312–322. doi: 10.1111/j.1574-6941.2012.01299.x
- Rippka, R. (1988). “[1] Isolation and purification of cyanobacteria.” *Methods in Enzymology*. (Academic Press) 167, 3–27. doi: 10.1016/0076-6879(88)67004-2

- Roberts, P., Hamilton, R., and Piperno, D. R. (2021). Tropical forests as key sites of the "Anthropocene": past and present perspectives. *Proc. Natl. Acad. Sci. USA* 118, 1–7. doi: 10.1073/pnas.2109243118
- Rocha, F., Lucas-Borja, M. E., Pereira, P., and Muñoz-Rojas, M. (2020). Cyanobacteria as a nature-based biotechnological tool for restoring salt-affected soils. *Agronomy* 10, 1–15. doi: 10.3390/agronomy10091321
- Sanseverino, I., António, D. C., Loos, R., and Lettieri, T. (2017). *Cyanotoxins: methods and approaches for their analysis and detection*. Available at: <https://ec.europa.eu/jrc>.
- Silva, C. S. P., Genuário, D. B., Vaz, M. G. M. V., and Fiore, M. F. (2014). Phylogeny of culturable cyanobacteria from Brazilian mangroves. *Syst. Appl. Microbiol.* 37, 100–112. doi: 10.1016/j.syapm.2013.12.003
- Staley, J. T., Konopka, A., and Staley Allan, J. T. K. (1985). Microorganisms in aquatic and terrestrial habitats. *Annu. Rev. Microbiol.* 39, 321–346. doi: 10.1146/annurev.mi.39.100185.001541
- Strunecký, O., Ivanova, A. P., and Mareš, J. (2023). An updated classification of cyanobacterial orders and families based on phylogenomic and polyphasic analysis. *J. Phycol.* 59, 12–51. doi: 10.1111/jpy.13304
- Tamminen, M., Spaak, J., Tlili, A., Eggen, R., Stamm, C., and Räsänen, K. (2022). Wastewater constituents impact biofilm microbial community in receiving streams. *Sci. Total Environ.* 807, 1–8. doi: 10.1016/j.scitotenv.2021.151080
- Tan, L. T., and Phyto, M. Y. (2020). Marine cyanobacteria: a source of lead compounds and their clinically-relevant molecular targets. *Molecules* 25, 1–30. doi: 10.3390/molecules25092197
- Townson, S., Connelly, C., Dobinson, A., and Muller, R. (1987). Drug activity against *Onchocerca gutturosa* males *in vitro*: A model for chemotherapeutic research on onchocerciasis. *J. Helminthol.* 61, 271–281. doi: 10.1017/S0022149X00010178
- Trang, N. T., Anh, T. T. N., Khanh, L. N., Hang, T. T., Loan, N. T. B., Anh, T. T. T., et al. (2021). Isolation of cyanobacterial strains from water and soil samples in hanoi and investigation of their cytotoxic activity. *VNU J. Sci. Nat. Sci. Technol.* 37, 26–36. doi: 10.25073/2588-1140/vnunst.5297
- Vitorino, L. C., and Bessa, L. A. (2018). Microbial diversity: the gap between the estimated and the known. *Diversity* 10, 1–29. doi: 10.3390/D10020046
- Wang, M., Carver, J. J., Phelan, V. V., Sanchez, L. M., Garg, N., Peng, Y., et al. (2016). Sharing and community curation of mass spectrometry data with global natural products social molecular networking. *Nat. Biotechnol.* 34, 828–837. doi: 10.1038/nbt.3597
- Wang, E., Sorolla, M. A., Krishnan, P. D. G., and Sorolla, A. (2020). From seabed to bedside: a review on promising marine anticancer compounds. *Biomolecules* 10, 1–59. doi: 10.3390/biom10020248
- Welker, M., and Von Döhren, H. (2006). Cyanobacterial peptides - nature's own combinatorial biosynthesis. *FEMS Microbiol. Rev.* 30, 530–563. doi: 10.1111/j.1574-6976.2006.00022.x
- Wu, L., Yang, P., Luo, L., Zhu, W., Hong, Y., Tong, C., et al. (2022). Conversion of mangrove forests to shrimp ponds in southeastern China destabilizes sediment microbial networks. *Geoderma* 421, 1–13. doi: 10.1016/j.geoderma.2022.115907
- Zaheri, A., Bahador, N., Yousefzadi, M., and Arman, M. (2021). Molecular identification and toxicity effects of cyanobacteria species isolated from the Koor-e-Khooran mangrove forest, Persian Gulf. *Iran. J. Fish. Sci.* 20, 572–589. doi: 10.22092/ijfs.2021.123905
- Zhang, X., Chen, Z., Yu, Y., Liu, Z., Mo, L., Sun, Z., et al. (2022). Response of bacterial diversity and community structure to metals in mangrove sediments from South China. *Sci. Total Environ.* 850, 1–10. doi: 10.1016/j.scitotenv.2022.157969
- Zhu, L., Zancarini, A., Louati, I., De Cesare, S., Duval, C., Tambosco, K., et al. (2016). Bacterial communities associated with four cyanobacterial genera display structural and functional differences: Evidence from an experimental approach. *Front. Microbiol.* 7. doi: 10.3389/fmicb.2016.01662
- Zubia, M., Turquet, J., and Golubic, S. (2016). Benthic cyanobacterial diversity of Iles Eparses (Scattered Islands) in the Mozambique Channel. *Acta Oecol.* 72, 21–32. doi: 10.1016/j.actao.2015.09.004
- Zubia, M., Vieira, C., Palinska, K. A., Roué, M., Gaertner, J. C., Zloch, I., et al. (2019). Benthic cyanobacteria on coral reefs of Moorea Island (French Polynesia): diversity response to habitat quality. *Hydrobiologia* 843, 61–78. doi: 10.1007/s10750-019-04029-8